Universidade do Porto
Faculdade de Engenharia
FEUP

Master in Chemical Engineering

Department of Chemical Engineering

Influence of different electrolyte compositions and a cathode protective layer on the performance of lithium–sulfur batteries

Master´s Thesis

by

Ana Luísa Pires Baltazar

Developed in the course unit of Dissertation

performed in

DLR- Institute of Technical Thermodynamics

Deutsches Zentrum
DLR für Luft- und Raumfahrt e.V.
in der Helmholtz-Gemeinschaft

Supervisor at FEUP: **Profª Alexandra Pinto**

Supervisor at DLR: **Natalia Cañas**

July, 2012

Acknowledgments

In this work there were several people who contribute in one form or another for its development. In first place for all the enthusiasm, friendliness, concern, and support during every difficulty during the work, I would like to thank to my supervisor at DLR, Natalia Cañas. I also would like to acknowledge my supervisor at Feup, Alexandra Pinto, for all the interest and support showed, even by distance it was very helpful. I acknowledge Norbert Wagner to give the possibility to do my master thesis in his group in DLR and for the nice work atmosphere. I also want to show my appreciation to Kei Hirose who taught me the first steps to make a battery. At last but not least I wanted to show my gratitude to my family, friends and especially to Sofia Félix who shared this adventure of going in the Erasmus program with me and who has been very supportive since the first day. Also to my boyfriend Joao Esteves who has always been supporting me to study abroad.

A special acknowledgment to Ina Plock and Natalia Cañas who performed all the SEM and XRD tests, respectively.

I would like to show my gratitude to Serviços de Acção Social da Universidade do Porto (SASUP) for giving the financial support then providing this great opportunity. Finally, a special acknowledge to the professors Miguel Madeira and Adélio Mendes for establishing contact with DLR and for giving the enthusiasm and support to participate in this Erasmus internship program.

Abstract

Nowadays lithium sulfur batteries are one of the main subjects of the battery research community. This is because of its high specific capacity, high energy density, low cost and eco-friendly materials that are used for its fabrication. Nevertheless, this battery type presents high degradation during cycling and more investigation focused on new materials and electrolytes has to be performed.

In this work, three main topics were studied: $LiNO_3$ as an additive for the electrolyte, a polymeric protective layer for the cathode and ultrasound mixing for the cathode suspension preparation.

The ultrasound mixer, for the suspension preparation, was tested in order to decrease the time needed with the traditional/mechanical mixer. The decreasing of time was successfully achieved. However, this mixer presented many disadvantages, such as agglomerates formation and loss of active material. The batteries showed poor cycling life, similar to the standard batteries (mechanical mixer). In the second part of this work two protective layers were created with different concentrations of an ion conductive material (LiCGC) with PVDF. These layers were studied by means of SEM, XRD and electrochemical cycling. The layer with less concentration of LiCGC showed great stability upon cycling. The capacity loss between the 2^{nd} and the 50^{th} cycle for the batteries with this layer was 30 %. For the layer with higher concentration of LiCGC was 79% and for the batteries with no protective layer was 55%. In the last part of this work, the influence of $LiNO_3$ as an additive to the standard electrolyte (1 M of $LiPF_6$ in TEGDME) was studied. For concentrations lower than 0,1 M of $LiNO_3$ the shuttle mechanism was not avoided as the batteries had charge-discharge efficiencies lower than 100%. From 0,1 M to 1 M the batteries showed great stability and higher capacity when comparing to the standard batteries. The optimal concentration found for the electrolyte additive was 0,75 M. With this electrolyte capacities of 536 Ah/kg were achieved after 50 cycles.

Key words: Lithium sulfur batteries, *shuttle mechanism, lithium polysulfides, cathode protective layer, $LiNO_3$*

Declaração

Declara, sob compromisso de honra, que este trabalho é original e que todas as contribuições não originais foram devidamente referenciadas com identificação da fonte.

Table of Contents

List of Figures

List of tables:

Glossary

List of relevant units

Ah/kg	**Specific capacity (kg refers in this work to the mass of sulfur)**
I	**Current**
V	**Voltage**
Wh/kg	**Specific energy (kg refers in this work to the mass of sulfur)**
A/kg	**Current density**
M (mol/L)	**Molar Concentration**

List of chemicals

LiCGC	**Lithium ion conductive glass ceramic**
DMSO	**Dimethyl sulfoxide**
PVDF	**Polyvinylidene fluoride**
CB	**Carbon black**
TEGDME	**Tetraethylene glycol dimethyl ether**
PEG	**Polyethylene glycol**
$LiPF_6$	**Lithium hexafluorophosphate**
$LiNO_3$	**Lithium nitrate**
$Li_4(P_2S_6)$	**Lithium phosphorus sulfide**
LiF	**Lithium fluoride**

1. Introduction

1.1 Background and Project Presentation

For the last past years the world has faced some several problems concerning the limited carbon fuels resources. The increasing price of these resources as led to demand for other options like renewable energies such as wind, wave, solar energy and their application in different fields. With the production of oil predicted to decline, the increasing number of vehicles and the pollution impact they bring, it has become necessary to change our transportation economy in order to protect the environment and our life quality. For this purpose, we need batteries with a higher specific energy capacity for the electrical mobility. One of the most promising candidates for energy storage is the lithium-sulfur battery. In contrast with lithium ion conventional batteries, which operate on the basis of intercalation reactions and have a specific energy density of 150-200Wh/kg, the lithium-sulfur batteries offer a much higher specific energy density 2500Wh/kg and a theoretical capacity of 1675mAh/g. In order to overcome these problems, it is necessary to understand the degradation mechanisms of these batteries and new materials and technologies have to be investigated.

In this work, a cathode protective layer based on a mixture of an ion conductive material, lithium ion conductive glass ceramics (LiCGC) and a polymer polyvinylidene fluoride (PVDF) was created to enhance sulfur retention and avoid morphological changes. The influence of $LiNO_3$ on the cycle stability of Li-S batteries was also investigated. This additive to the electrolyte was tested for different concentrations. In addition, the performance of ultrasound and mechanical mixing conditions during the suspension preparation were compared.

1.2 Deutsches Zentrum für Luft- und Raumfahrt - DLR

DLR is Germany's national research center for aeronautics and space. Its areas of researching include aeronautics, space, transportation and energy and it provides international representation of German´s interests. DLR's mission comprises the exploration of the Earth and the solar system but also focuses its research on the protection of the environment by developing new environmentally friendly technologies for the mobility, communication and security.

This company is responsible for providing a job to approximately 7000 people who are divided in 32 institutes and facilities at 16 locations in Germany. DLR also has offices in Brussels, Paris, Singapore, and Washington D.C. It works in large scale facilities and it promotes the next generation of researchers.

1.2.1 DLR Institute of Technical Thermodynamics

This institute lies on the field of researching of efficient energy storage systems that conserve natural resources, providing and sustainably development of the countries. This Institute comprises a staff around 150 scientific and technical employees, engineers and doctoral candidates. The Institute of Technical Thermodynamics also works on selected subjects from the fields of 'Aviation' and 'Transportation', thus contributing to other focal points of DLR. These include developments to the use of fuel cells in aircraft and ground vehicles and to the generation and storage of hydrogen. The Institute and its activities are very well integrated in national and international research networks. Due to the fields in which it researches, the institute acts as a bridge between basic research and industrial development, and thus often plays a key role in the introduction of new technologies. In addition to research and development, other important functions are advising political and business decision-makers, and advanced training of young scientists.

1.2.1.1 Battery Technology

The "Battery Technology" group focuses its research on the development of new generation of Li-Batteries: Li-Sulfur and Li-Air Batteries, because of their theoretical high capacity and energy densities. In spite of these advantages these batteries still present many challenges that need to be overcome in order to obtain good results. For this matter, this group works with the objective of obtaining reliable batteries using safe materials. Some other research activities of the group include:

- Investigation of degradation processes on the new generation of batteries
- Determination of status of battery with in-situ diagnostics and frequency analysis
- Multi-scale-modeling and simulation of electrochemical processes in the batteries
- Long term cyclization

The group test and characterize not only the self-fabricated batteries but also commercial batteries. For this purpose, the following measurement devices are available:

- Test stations for batteries from mW to kW with climate chambers and electrochemical impedance spectrometer (EIS)
- Test stations for half-cell measurements

- Test station for rotating disc ring electrode
- In-situ and ex-situ XRD
- Optical spectroscopy (IR- and Raman spectroscopy)
- XPS
- Adiabatic Calorimeter
- Porosimeter

1.3 Contributions of the Work

This work has done the following contributions to the development of Li-S Batteries in the "Battery Technology" group of DLR:

- testing the applicability of ultrasound mixer for the preparation of the cathode suspension
- first experiments for the fabrication of a protective layer for the cathode by means of an ion conductive polymeric layer
- Improving the capacity of the battery after 50 cycles with a new electrolyte composition

1.4 Thesis Organization

This work is organized in five principal chapters. Chapter 1, the present chapter, consists of the work presentation, summarizing the objectives and results of the project as well as a description of the host institution. Chapter 2 is an introduction to Li-S batteries including its advantages and problems and also comparison with the commercial batteries. Some previous research done in this field is also described. Chapter 3 is about the experimental work performed with a detailed description of materials and methods. Chapter 4 presents the results and discussion of the experimental work. In this chapter the most relevant results obtained from the measurements are shown. Chapter 5, the conclusions chapter, summarizes the results, whether successful or not, the accomplishment of objectives and also all the problems that need to be overcome. Furthermore a recommendation for the future work in this field is outlined.

2. Background and State of the Art

2.1 Lithium Sulfur battery

The lithium sulfur batteries are becoming more interesting for the use in electrical vehicles and in all the portable devices than lithium ions batteries because of their higher capacity and light weight. In these batteries the cathode comprises elemental sulfur normally mixed with electronic conductors to increase the electrical conductivity. In this electrode there can be several different composition including elemental sulfur, organo-sulfur, or carbon sulfur composition. The anode is normally composed with lithium metal but other materials with lithium can also be used for example, lithium foil, lithium alloys and lithium deposited into a substrate. The separator is normally porous and non- conductive and it has the function of insulating the cathode from the anode but at the same time it should allow that ions move through it (Mikhaylik, 2010). The electrolyte used in these batteries is normally organic and it can be either aqueous or nonaqueous and its function is to transport and store the ions. It is also very important that the electrolyte does not react chemically and electrochemically with the material of the electrodes and that it is also non-conductive to prevent short circuit between the anode and the cathode. In the image below the Li-S battery is illustrated

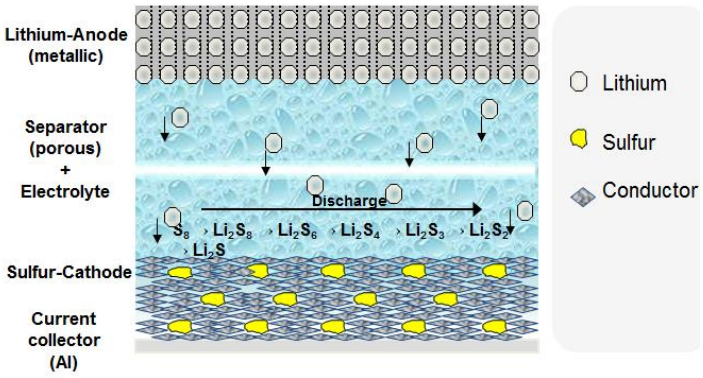

Figure 1: Scheme of Li-S battery

2.1.1 Reactions

It is known that polysulfides (Li_2S_x x=1-8) are formed as intermediates as result of electrochemical processes occurring in lithium-sulfur batteries during charge and discharge. These components are formed from the reduction of S_8 to S_8^{2-}, S_6^{2-}, S_4^{2-}, S_2^{2-} and finally to S^{2-} during discharge. However the number of stable intermediate sulfides is still yet to be found. They are soluble in the majority of aprotic dipolar solvents and electrolytic systems based on them.

The electrochemical reduction of sulfur during discharge and the oxidation of the products of this reduction during charge occur in two stages as it can be seen in the image represented by two different plateaus (Karaseva, 2006).

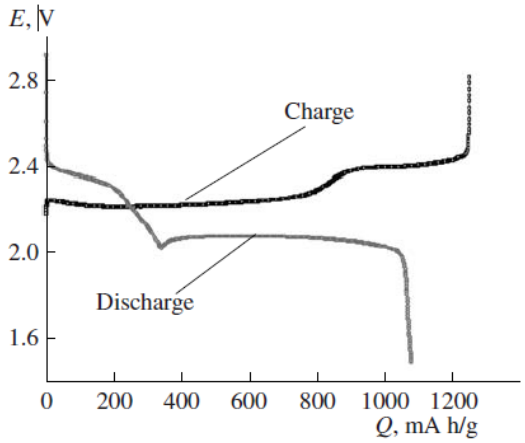

Figure 2: Discharge and charge plateaus upon cycling (Karaseva, 2006)

The first plateau occurring between 2,5-2,0V corresponds to the reduction of elemental sulfur into lithium octasulfide (1) which is soluble in electrolytes. In this stage the voltage change is relatively high compared to the voltage change in the second stage. The reaction kinetics in the first stage is fast owing to the molecular nature of the species involved (F.Nazar, 2010). The next reaction is a simplification of this reduction.

$$S_8 + 2e^- + 2Li^+ \rightarrow Li_2S_8 \quad (1)$$

$$Li_2S_8 \rightarrow Li_2S_n + (8-n)S \quad (2)$$

The second stage of Li-S batteries is the reduction of lithium polysulfides dissolved in the electrolyte. The mechanism of this step is not very well known but it is going to be explained based on (Karaseva, 2006). First the reduction of sulfur polysulfides into polysulfides of lower chain length occurs. This can be resumed by the following reactions.

$$Li_2S_n + 2e^- + 2Li^+ \rightarrow Li_2S\downarrow + Li_2S_{(n-1)}, \quad (3)$$

$$Li_2S_{n-1} + 2e^- + 2Li^+ \rightarrow Li_2S\downarrow + Li_2S_{(n-2)}, \quad (4)$$

$$Li_2S_2 + 2e^- + 2Li^+ \rightarrow 2Li_2S\downarrow; \quad (5)$$

After these reactions it is verified a decreasing in the concentration of polysulfides in the electrolyte.

$$Li_2S_n + 2e^- + 2Li^+ \rightarrow Li_2S \downarrow + LiS_{(n-1)}, \quad (6)$$

$$xLi_2S_{n-1} \rightarrow Li_2S \downarrow + yLi_2S_n \quad (7)$$

In this step the final product is the insoluble Li_2S. This step is the most difficult and slow because of the energy that is needed to form this product and the sluggishness of solid state diffusion in the bulk.

The charge of lithium sulfur batteries also occurs in two stages but is much simpler. According to (Karaseva, 2006) the first medium chain lithium polysulfides are reduced to long chain ones. This process can be described by the following reaction.

$$mLi_2S_k - 2e^- - 2Li^+ \rightarrow gLi_2S_n, \text{ where } mk = gn \quad (8)$$

The resulting long chain polysulfides react with short chain lithium polysulfides producing medium chain lithium polysulfides. Then these are oxidized to long chain lithium polysulfides. This process continues until the concentration of polysulfides decreases (almost until zero) and they together form elemental sulfur in the potential range of 2,4-2,6V.

When polysulfides dissolve in the electrolytes they can increase the viscosity and decrease the electric conductivity. As the viscosity of electrolyte solutions of Li-S batteries increases, electrochemical reactions are displaced from the bulk of the electrode to its surface. This mechanism makes thick porous electrodes unusable for Li-S batteries. The change in the electrolytes can affect severally the electrochemical process in the lithium-sulfur cells.

2.1.2 Advantages

The lithium-sulfur batteries are one of the most interesting options for the storage of energy as they offer high specific energy density 2500Wh/kg and a theoretical capacity of 1675mAh/g. As they use the sulfur as a positive electrode they can achieve high energy densities due to its capacity of reaction with metallic lithium to form Li_2S with a two- electron reaction. This means that all Li atoms in anode and S atoms in cathode are subjected to oxidation/reduction. Besides, sulfur has an advantage of natural abundance, light-weight, low cost, environmental friendliness, wide temperature range of operation, intrinsic protection mechanism to overcharge and possibility of long cycling. It is also known that Li-S batteries do not suffer from memory effect and they are very tolerant to overcharging.

2.1.3 Disadvantages

Despite of its considerable advantages they also have some associated problems to overcome due, under other reasons, to the fact that sulfur is an insulator (electrical conductivity: $5x10^{-30}$ S/cm at 25 °C (Dean, 1985). To avoid a reversible electrochemical reaction the sulfur must be in contact with high

amounts of electrically conductive additives (for example: graphite, Carbon Black). The sulfur also has poor recharge ability due to the loss of active material during the charge and discharge process. This is one of its biggest problems since it leaves to a degradation of the battery capacity. This degradation is related to the high solubility of the polysulfides. These polysulfides contribute to the "shuttle" mechanism which leads to an active mass loss and to a morphological change in the cathode. In addition the solid product that is constantly formed in the cathode precipitates on the surface, during discharge, causes the build-up of impedance layers which results in capacity fading.

2.1.4 Shuttle Mechanism

One of the most difficult problems to overcome in this type of batteries is the shuttle mechanism. This mechanism occurs because of the high solubility of the polysulfides of higher order (Li_2S_x x $>$2) formed on the reduction of S_8 or upon the oxidation of the end member sulfides. These species diffuse in the electrolyte and migrate through the separator to the anode where they are reduced to insoluble Li_2S or Li_2S_2. When the anode is fully coated, the following S_n^{2-} react with these fully reduced sulfides to form lower order of polysulfides which become concentrated at the negative electrode side. After, they diffuse to the positive electrode and are then re-oxidized into S_n^{2-}. This process is most known as a shuttle mechanism and it contributes to the decreasing of active mass utilization in the discharge process and reduces de Coulombic efficiency in the charge process (F.Nazar, 2010).

2.1.5 Comparison with commercial batteries

The lithium sulfur batteries have received a stronger attention due to its high theoretical specific energy density which is 3 to 5 times higher than the lithium ion batteries. The lithium ion battery is a rechargeable battery in which lithium ions move from the negative electrode to the positive electrode during discharge and back during charge. They use an intercalated lithium compound as electrode material instead of metallic lithium contributes to a lower energy density about 300 mAh/g in these batteries. The anode is normally carbon and the most widely used cathode is cobalt oxide. The fact that Li-S batteries use pure lithium as the anode material is what allows these batteries to have a high specific capacity. In comparison with lithium ion batteries, Li-S batteries are safer because lithium dendrites do not form here. (F.B. Tudron, 2004).

Li-S batteries have a lower voltage (approximately 2,1 V) then the Li ion battery (approximately 3,8 V). This can also be better for the new trends of consumer electronic products.

At the present, with the increasing development of technology for electrical vehicles and portable devices, the Li ion battery is limited with its energy capacity. For this reason, the actual intercalation

chemistry has to be replaced for a new technology. A promising trend is the integration chemistry used in lithium air and lithium sulfur batteries.

2.1.6 State of Research

The lithium sulfur batteries have been a large subject of testing for the last past years. Because of their high theoretical capacity and the many challenges they bring, the researchers have been trying several modifications at all levels. There can be changes at level of chemistry or in the physics of the cells. The changes in chemistry can be in the electrodes, in the electrolyte or in the separator. The changes in the physics of the cells can be, for example, pressed cathodes. This part of the work will present some of the advances that have been made so far in the Li-S batteries field.

2.1.6.1 Cathodes

Several carbonaceous materials are used within the cathode to increase the conductivity of this electrode but at the same time it is verified that the energy density decreases. For this matter different configurations of carbon within the cathode have been created. The first cells with carbon in their composition were just a mixture of bulk carbon and sulfur powder. These cells had low capacity and low cycling life (F.Nazar, 2010). More recently, activated carbon was applied because of its high surface area, pore volume and cost-effectiveness. However, this material has a high range of size distribution (<2nm to >50nm) which leads to a poor contact surface between sulfur and carbon (F.Nazar, 2010). In the last decade the multi walled carbon nanotubes (MWCNT´s) have been causing a significant impact as they present excellent electrical, thermal and mechanical properties. They can obtain high reversible capacities and as nano-materials can provide high surface area and high surface to volume ratio. They can also provide high kinetic activity and supply sufficient contact interface between sulfur and the electrolytes (Jia-jia Chen). In spite of the considerable advantages of these carbon nanotubes they still present big challenges as it is difficult to obtain good contact between sulfur and MWCNT and also to disperse sulfur homogenously due to the small tubes size. Normally these carbon nanotubes act as wires to conduct and encapsulate the sulfur inside a network. (Jia-jia Chen) also studied S/MWCNT nanomicrosphere with large pores obtaining a reversible capacity of 1000 mAh/g after 100 cycles at 0,3 A/g and showing a significant cyclability enhancement. They also changed the nano structure of S/MWCNT adding nitric acid so that the sulfur could be uniformly coated on its surface by solvent exchange method. Most recently the mesoporous carbons have been used to contain sulfur as an ordered interwoven carbon sulfur composites that comprise high pore-volume carbons. Sulfur is incorporated from the melt by capillary forces. This method eases the control of active mass present in the system (F.Nazar, 2010). The polymer modification of the carbon surface also contribues to a

complete reaction because it retards the diffusion of polysulfides into the electrolyte. In the image below is illustrated an example fo this structure.

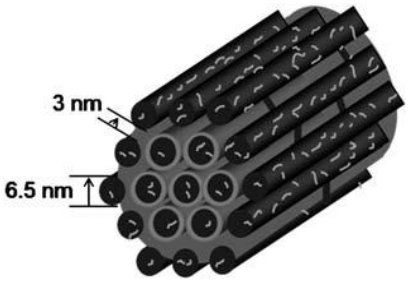

Figure 3: Scheme of polyethylene glycol (PEG200) with coating of mesoporous carbon (CMK-3S) composites (F.Nazar, 2010)

2.1.6.2 Cathode/anode protective layer

Some researching in turn of building a protective layer for the electrodes has been made in order to avoid the shuttle mechanism. In this field, several attempts are being made to achieve higher capacity and stability in the batteries cycling. (Jusef Hassoun, 2012) has built a protective layer for the cathode by annealing sulfur and pitch carbon followed by mechanical treatment. After, they also covered this with a thin layer of thin nickel metal by means of electron beam physical vapor deposition (EBPVD). With this procedure they achieved capacity retention and more cycling stability by decreasing the concentration of lithium polysulfides in solution. In the following image one of the results from this work is presented. As it can be seen the decrease in capacity is almost zero from the third to the fifty cycle.

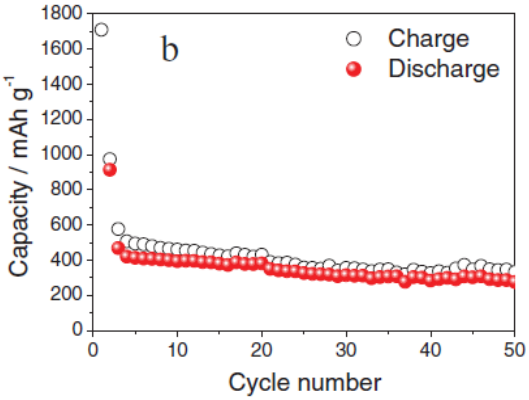

Figure 4: Capacity variation with the cycle number for the nickel layer covering sulfur-carbon sample (Jusef Hassoun, 2012)

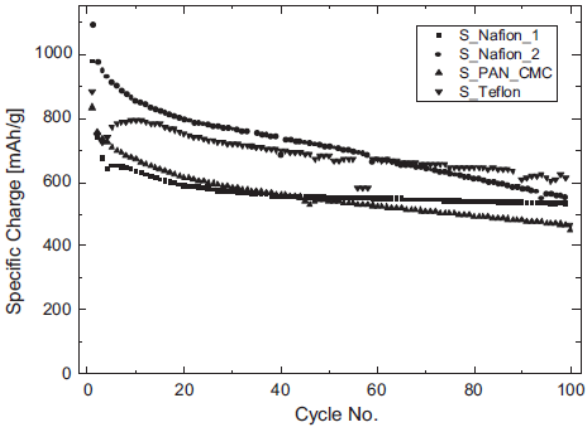

Figure 5: Specific charge upon cycling of electrodes employing Nafion as a binder material (S Nafion 1 and S Nafion 2), a polyacrylonitrile/ carboxymethylcellulose composite (S PAN CMC), and Teflon (S Teflon) (Rate: C/10, all curves are averages over several experiments). (Holger Schneider, 2011).

(Holger Schneidera, 2012) also tested Nafion as a coating material for the cathode (Holger Schneider, 2011). They studied Nafion, polyacrylonitrile/carboxymethylcellulose and Teflon as binders but only the batteries with Nafion had an extra sprayed Nafion layer (S_Nafion_2) that worked as coating. In result, a good cycling performance and stability was achieved (see Figure 5). It is believed that the Nafion cationic exchange properties contribute to sulfur insulating by inhibition of the reactions between the polysulfides.

2.1.6.3 Electrolytes

Many changes have been made at the electrolyte level. This is due to the fact that this component is one of the most important in the battery composition as its function is to conduct the ions. For this matter, changes in this element contribute to significant changes in the battery performance. Several different electrolytes have been tested with significant change in the battery capacity. (Duck-Rye Chang, 2002) tested a electrolyte that is a mixture of tetra(ethylene glycol) dimethyl ether (TEGDME) with 1,3-dioxolane (DOXL). The maximum value of the conductivity achieved was for a ration of TEGDME: DOXL of 30:70 due to the fact that DOL reduces the viscosity of the electrolyte medium. In the other hand this viscosity values were difficult to control and the utilization of sulfur was very low. (Weikun Wang, 2009) investigated lithium perchlorate in 1,3-dioxolane and dimethylethane ($LiCLO_4$ DOL/DME) as electrolyte. They discovered that high content of DME can increase the resistance of the battery due to the polysulfides dissolution. The optimal results were with a composition of DME:DOL, 2:1. With this composition the initial capacity of the batteries were 1200 mAh/g and after 20 cycles it still close to 800 mAh/g.

More recently, lithium nitrate has been investigated as an additive to the electrolyte. (Mikhaylik, 2010) tested several concentrations of this additive improving the charge capacity and the charge - discharge

efficiency. They studied several different concentrations of this additive in a electrolyte solution of lithium imide in a 50:50 ratio mixture of 1,3-dioxolane (DOL) and dimethoxyethane (DME). They also tested this additive in a solution of trifluoromethyl sulfonate. To prove that N-O chemical bond was the responsible for inhibition of the shuttle mechanism, they tested different components with this bond (potassium nitrate, cesium nitrate, ammonium nitrate, potassium nitrite, dinitro toluene). The higher charge - discharge efficiency and capacity upon cycling were achieved with $LiNO_3$ for the concentration range between 0,2 M to 1,0 M.

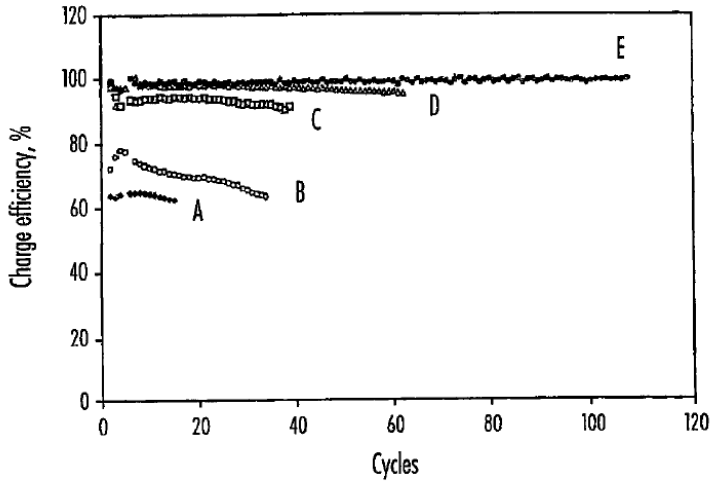

Figure 6: Curve of charge - discharge efficiency upon cycling. Curve A, represents the electrolyte with no additive; curve B the electrolyte with concentration of $LiNO_3$ of 0,002M; curve C the electrolyte with dinitro-toluene with 0,4M; D with 0,4M of $LiNO_3$; E with 1,55M of $LiNO_3$ (Mikhaylik, 2010)

Higher discharge capacities have been achieved by modifying both cathode and electrolyte. Guangyuan Zheng, 2011 studied hollow carbon nanofiber-encpasulated sulfur cathode that traps the polysulfides within them. The hollow carbon nanofiber arrays were built with anodic aluminum oxide (AAO) by means of thermal carbonization of polystyrene. These templates prevent that sulfur deposits in the carbon surface. The capacity upon cycling was of 730 mAh/g at C/5 rate after 150 cycles of charge/discharge (Mikhaylik, 2010).

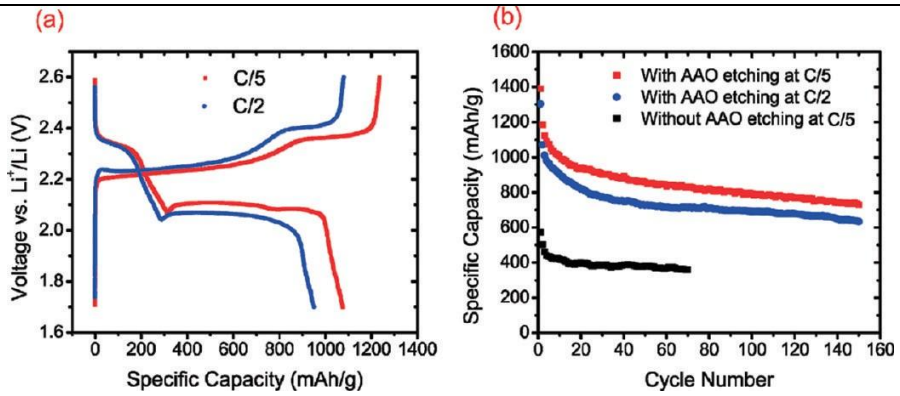

Figure 7: a) Typical charge and discharge voltage profiles; b) the capacity upon cycling with and without (AAO) (Guangyuan Zheng, 2011)

They also tested $LiNO_3$ as additive to the electrolyte with a concentration of 0,1 M, achieving high Coulombic efficiencies (Guangyuan Zheng, 2011).

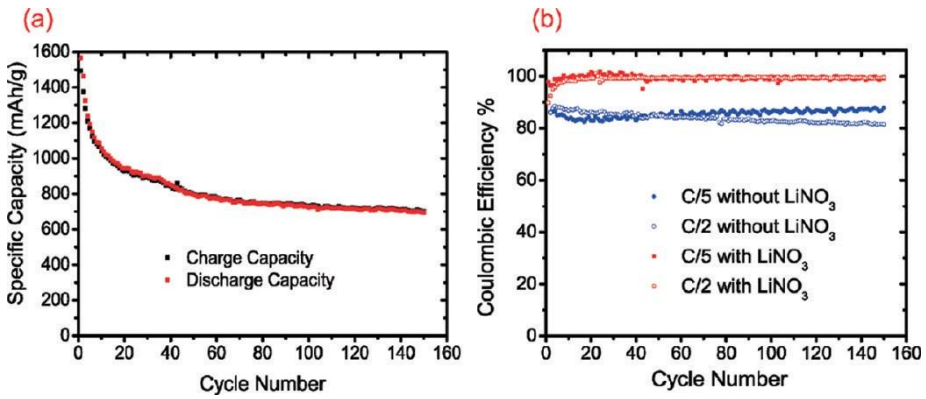

Figure 8: (a) curves of charge and discharge capacities upon cycling; (b) Couloumb efficiency upon cycling with and without $LiNO_3$ additive (Guangyuan Zheng, 2011)

3. Experimental work

3.1. Battery preparation

3.1.1 Cathode

3.1.1.1 Composition

The experimental work began with the preparation of the suspension for the cathode. This suspension contained about 50% of sulfur (Sigma Aldrich 99,98%), 40% of Carbon black, Super P® Conductive (Alfa Aesar 99%) and 10% of polyvinylidene fluoride (PVDF) from the company Sigma Aldrich, dissolved in Ethanol Absolut (Th.Geyer Chem Solute) and in dimethylsulfoxide (DMSO)(VWR ProLab 99,6%) with a composition of (60:40). Polyethylene glycol (PEG) from the company Sigma Aldrich was used as plasticizer in a percentage of 0,07.

Carbon black was used in this work as a conductive material to mix with sulfur. It has also high purity and high electrical conductivity due its chain-like structure. The low particles size of Carbon Black (ca.79 nm) benefits the coating of the bigger sulfur particles (ca.39 µm). PVDF acted as medium to link the carbon black and sulfur particles as it is a plastic material and presents high resistance to solvents. The size of these binding particles are spheres of 200 nm but in solution they can build particles from 2-20nm (see Figure 9 d). DMSO was used to dissolve PVDF because it is a polar aprotic solvent that dissolves in polar and nonpolar compounds and it is also miscible in a wide range of organic solvents. Ethanol was used for accelerating the drying process during spray as it is very volatile. Figure 9 shows the SEM images for carbon black, sulfur, PVDF, the separator Celgard® 2500 and Al-substrate from the company Showa Denko.

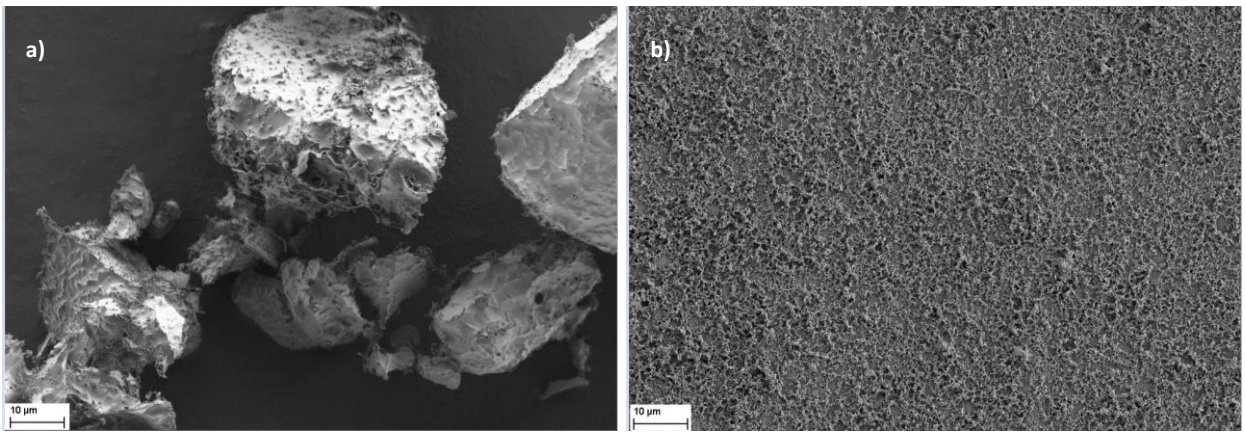

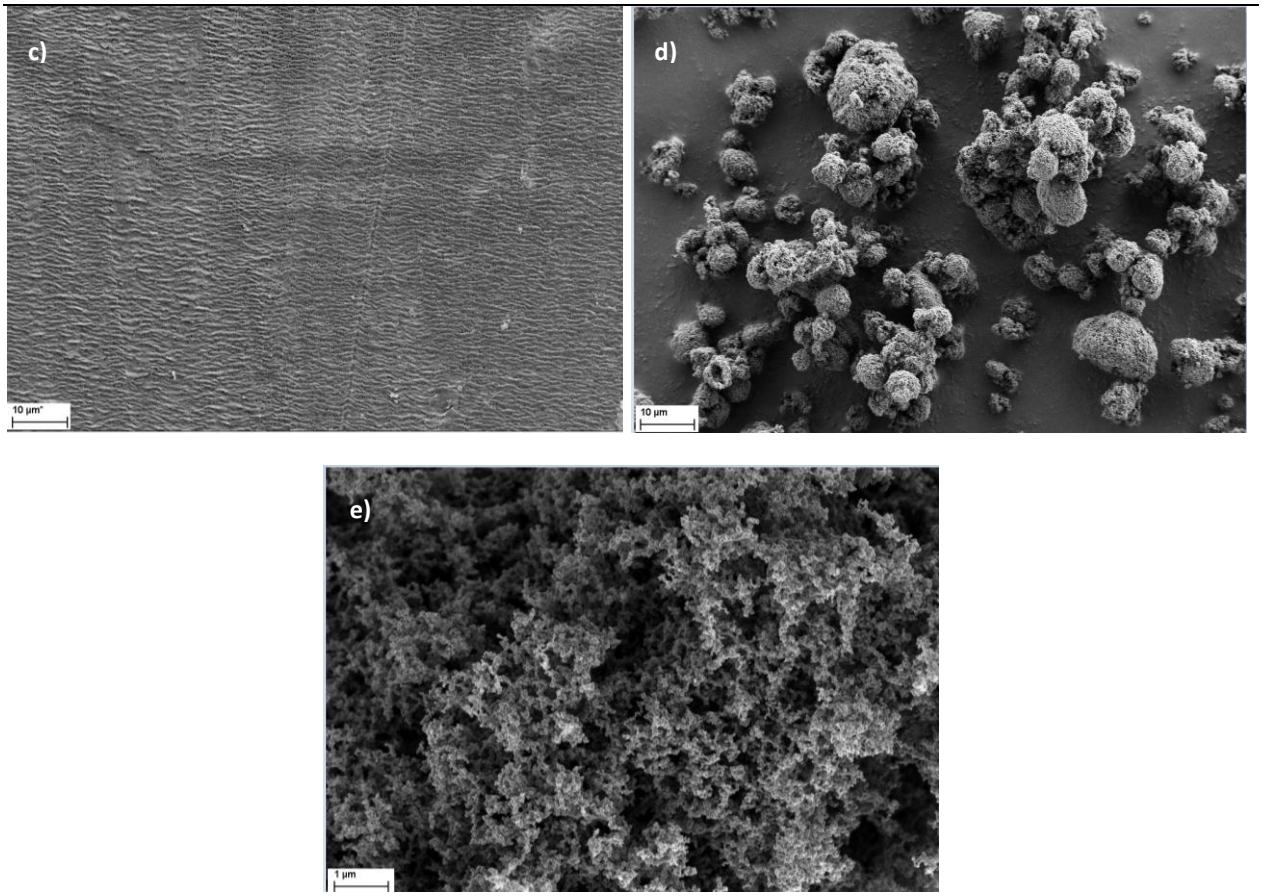

Figure 9: a) Sulfur particles; b) substrate with particles of carbon in aluminum foil; c) separator Celgard 2500; d) particles of PVDF; e) particles of carbon black.

3.1.1.2 Mixture procedure

3.1.1.1.1 Mechanical mixing

A tumbling mixer was used for mechanical mixing of the suspension. To increase the mixing behavior ceramic spheres were added to cause collision between the particles. This also helped to eliminate agglomerates in the suspension and decrease the sulfur particles size. For this mixing procedure, sulfur and carbon black powder were mixed together in the tumbling mixer for about 12 hours in order to obtain a homogeneous suspension. DMSO and ethanol were added to PVDF and subjected to magnet mixing for about 30 minutes to promote a better dissolution of the PVDF. PEG was added to this mixture after PVDF was completely dissolved. Finally, all the components were mixed together in the tumbling mixer.

3.1.1.1.2 Ultra sound mixing

Another type of mixing procedure was tested in order to decrease the mixing time of the suspension. This ultra sound mixing is normally known as sonication that is the act of applying sonic waves to agitate

the particles in the solution. Basically these waves lead to a disintegration of the particles by breaking intermolecular interactions. This type of mixing can be as an ultrasonic bath or an ultrasonic probe as used in this work. Figure 10 shows the ultra sound mixer with the ultrasonic probe.

Figure 10: Ultra sound mixer with ultrasonic probe (UP200s) from the company Hielscher- ultrasound technology

To evaluate this system, the influence of two parameters was tested: amplitude and time of mixing. For all tests, the time between waves was constant (0,5 s). Table 1 shows the different tests performed (A-I) with different Time-Amplitude combinations. After each test, the ultra sound was stopped, in order to verify the temperature and to take samples to be analyzed by means of scanning electrode microscope (SEM).

Table 1*:* Set of suspensions obtained with time and amplitude variation

Time (min)	Amplitude		
	20	**60**	**100**
5	A	B	C
20	D	E	F
35	G	H	I

It was very important to measure the temperature because this parameter increases very fast at 100 amplitude and it can change the composition of the suspension due to the evaporation of volatile solvents. To control the temperature, the glass that contained the suspension was inside of a recipient with water and ice during mixing. The variation of the temperature before and after mixing was normally between 14 – 19°C but for the experiments with amplitude of 100 this difference was higher (16-29°C).

3.1.1.2 Spraying

The suspension was sprayed with a home-made suspension-spray machine on a carbon coated aluminum foil substrate. The beaker with the suspension was placed in a metal box that had to be well closed to maintain constant the pressure inside. A magnetic mixer was under it in order to avoid agglomerates formation and solid deposition. This metal box was connected to two plastic tubes: one connected to the air feed which is responsible to create overpressure in the suspension and the other connected to the mixing nozzle for spraying. There are two plastic tubes connected to the nozzle, one directly connected to the air feed (air pressure for spraying can be regulate here) and the other connected also to air but with the function of opening and closing the entrance of suspension. The suspension is mixed with pressurized air in an external part of the mixing nozzle. The machine can work in three different axes and with different programs that allows the spraying nozzle to change its velocity and axe.

Between the spraying of each layer, the cathodes were dried in the oven at 50°C until they were stable. At the end they were dried for two days to evaporate the solvents and eliminate humidity in the material.

Table 2: Conditions used when spraying the suspensions mixed with the ultra sound (US-1) and with the mechanical mixer

Sample ID	Air Pressure (bar)	Suspension overpressure (bar)	Layers	Speed (mm/s)
SA8-1	0,5	0,14	4	300
SA8-2	0,5	0,14	4	300
SA9-1	0,2-0,4	0,19	4	300
SA9-2	0,2-0,4	0,19	4	300
US-1	0,2-0,4	0,19	4	300

3.1.2 Protective layer

One of the main objectives of this work was to build a cathode protective layer to avoid the shuttle mechanism and morphological changes in the cathode. In order to avoid these problems a protective layer was built with the compositions presented on the following table. Lithium ion conductive glass ceramics (LiCGC) from the company OHARA INC was used as an ion conductive material to facilitate the transportation of the lithium ions as its conductivity is 10^2 S /m (www.ohara-inc.co, 2012). It also has good chemical resistance and it is not influenced by water or acids. The particles size is between 1-10 µm allowing a high dissolution. In the following table composition of the different layers can be seen.

Table 3: Composition of the different cathode protective layers and the ratio of the solvent and layer material

	L_a	L_b
Material		
PVDF	90	60
LiCGC	10	40
Solvent		
DMSO	60	60
Ethanol	40	40
Solvent : Layer Material	99:1	99:1

3.1.2.1 Mixing

The suspension for the protective layer was mixed with the tumbling mixer. In this case, a lesser time was needed when compared to the time for the normal cathode suspension (total time about 45 min).

3.1.2.2 Spraying

Before spraying the protective layer suspension over the already prepared cathodes, it was necessary to find an optimal air pressure and overpressure of the suspension, because of the difference in viscosity when compared to the suspension for the cathode. The main objective was to obtain a thin and homogeneous layer. To evaluate these two parameters, the first tests with this suspension were sprayed just in aluminum foil as it is easier to see the layer morphology when analyzing the results by means of SEM. All the next tests were performed over the normal cathode and over aluminum foil. Table 4 shows the different pressures used when spraying in the cathodes. In L_a the suspension overpressure was zero.

Table 4: Conditions used when spraying the protective layers

Sample ID	Air Pressure (bar)	Suspension overpressure (bar)	Layers	Speed (mm/s)
L_a	0,2-0,4	0	2	300
L_b	0,2-0,4	0,2	1	300

3.1.3 Electrolytes

Lithium nitrate (Sigma Aldrich) has been investigated as additive for a lithium ion conductive electrolyte composed of lithium hexafluorophosphate ($LiPF_6$) (Alfa Aesar, 99,99%) dissolved in tetra(ethylene) glycol dimethyl ether (TEGDME) (Sigma Aldrich 99%).

In Table 5, the composition of the different electrolytes tested is shown. The electrolytes were prepared in an argon atmosphere (inside the glove box) and then submitted to magnetic mixing until $LiNO_3$ and $LiPF_6$ were dissolved in TEGDME.

Table 5: Compositions of the different electrolytes used

Electrolyte	$LiPF_6$ (M)	$LiNO_3$ (M)
E_0	1	-
E_1	1	0,01
E_2	1	0,05
E_3	1	0,1
E_4	1	0,75
E_5	1	0,075
E_6	1	1
E_7	1	0,5
E_8	1	2

3.1.4 Swagelok cell

The main components of the cells are the cathode, with the composition mentioned before, separator, electrolyte and anode, lithium metal. In Figure 12, the different layers of the battery and also the thickness of each layer can be seen. The separator had a diameter of 1,2 cm to assure to avoid physical contact between anode and the cathode.

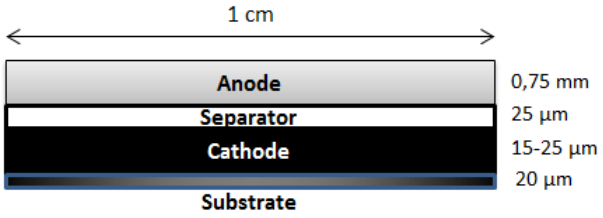

Figure 11: Scheme of the layers present in the battery and their thickness

The separator used was a 25 µm microporous monolayer membrane of polypropylene (Celgard® 2500). This separator was used because of its excellent resistance to most chemicals, uniform structure, thermal stability and high porosity providing high rate capabilities. The preparation of the cells was inside the glove box due to the high reactivity of lithium in contact with air and water. The atmosphere

of this system is composed mostly with argon with negligible concentrations of O_2 and H_2O. The complete battery was built in a Swagelok cell (

Figure 12). At first, a sample of 1 cm diameter was cut from the sprayed cathode with a hollow punch. Then it was weighed in order to calculate the quantity of sulfur in the cathode. This procedure was needed to find what charge/discharge current the battery was going to be submitted to in the BaSyTec.

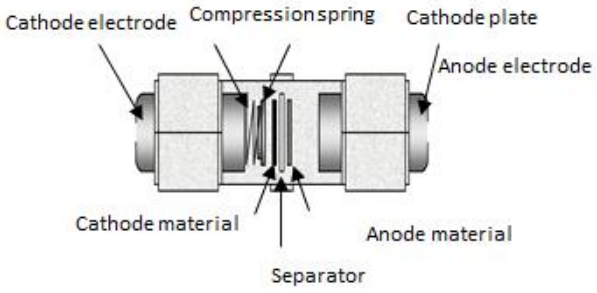

Figure 12: Representation of the Swagelok Cell

The cathode was placed in an aluminum plate over the spring as it can be seen in (Figure 12). This spring has the function of relieving the force that is applied when closing the battery. This also avoids the damage in the cathode when submitted to a high force. The next step was the addition of the electrolyte. At first, 7 ml directly in the cathode, then the separator, the other 7 ml and finally the lithium metal that was also cut with the hollow punch and placed over. Finally, the battery was closed with the help of screwdriver. Before taking the battery out of the glove box the open circuit voltage was measured with a voltmeter in CC before starting cycling in the BaSyTec. The open circuit voltage of the batteries was in the range of 2,5 – 3,5 V.

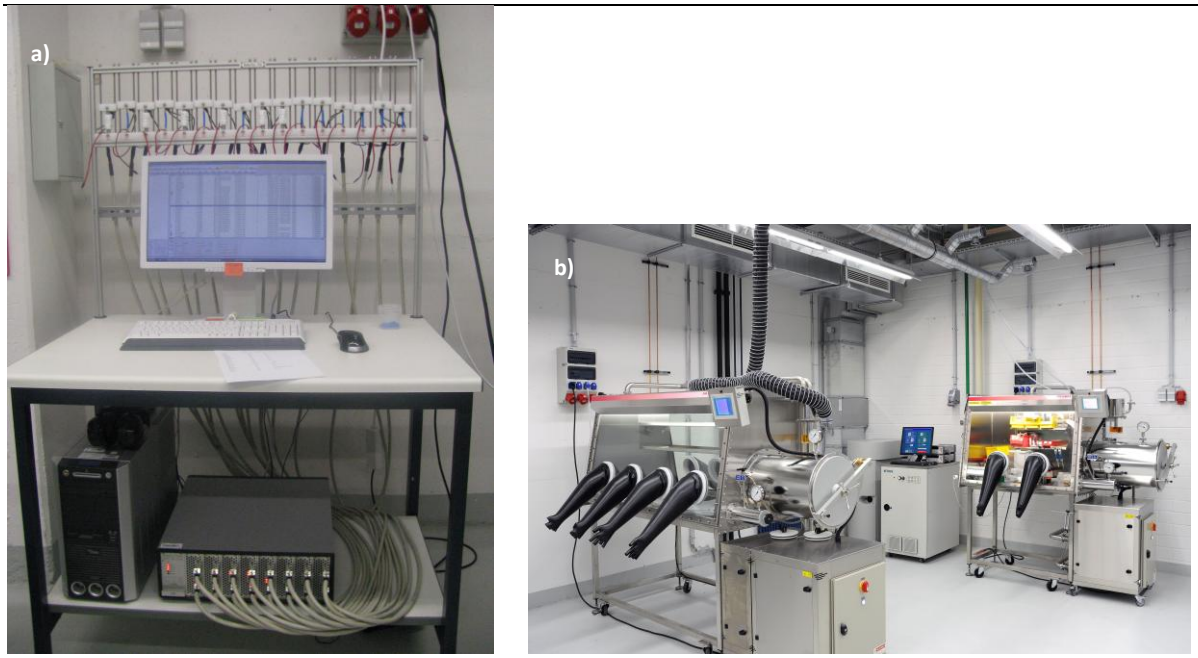

Figure 13: a) BaSyTec test equipment, with 16 channels to test batteries simultaneously. The batteries are testing in the top; b) Glove boxes used for the preparation of batteries.

3.2 Electrochemical characterization

3.2.1 Cycling of the batteries

The equipment used for cycling and testing the batteries was from the company BaSyTec. In this equipment the batteries were tested according to a plan that is predefined before starting cycling. The battery was charged galvanostatic with a current intensity of 500 A/kg. The end potential for charging and discharging was 2,8 V and 1,5 V, respectively. Only by charging the potential was maintained at 2,8V till the current decrease to 1/3 of the charge current or after 15 min of potentiostatic charge (which consists of holding the electric potential constant during the reaction using a potentiostat). This assures that the battery is completely charged before starting to discharge again. The batteries were tested until 50 cycles discharge, 50 cycles plus one charge or until 100 cycles. A maximum and minimum voltage was set for security reasons, in case the battery reached these values, the program shut off the battery. If the temperature got higher than 80°C the program stops the measurement in the channel. The values were measured each minute or when the potential change in 25mV.

With these measurements, the discharge and charge curves and the variation of the specific capacity with number of cycles can be plotted and analyzed.

3.2.3 Impedance measurements

Electrochemical techniques are very helpful to evaluate the batteries during charge and discharge as they present many advantages when comparing to other electrochemical techniques. They can measure the detailed kinetic values and also measure the battery properties under different usage and storage conditions. EIS is a very sensitive technique and it can provide analyses of the stage of charge, information about the reactions mechanisms, separator evaluation, identification of electrode corrosions and investigation of the kinetics of each process. Since the perturbation of alternating current (AC) signal is very small, the polarization of the electrode is in a linear potential region, this means that there is no destructive damage to the electrode.

Application of EIS technique is starting to be used in lighting and ignition (SLI), electric vehicle batteries, fuel cells and solid state batteries such as polymer electrolyte batteries.

In this work, impedance spectra of the batteries have been measured to compare the resistance contributions of the batteries by using different electrolyte composition. These batteries were tested with a potentiostat (ZAHNER®-Elektrik) and evaluated with the program Thales. The EIS measurements were performed in potentiostatic mode (voltage amplitude: 5mV) and in a frequency range between 60 mHz to 1 MHz.

3.3.1 SEM

Scanning electrode microscope (SEM) is a type of electron microscope that images a sample by scanning it with a beam of electrons. The electrons interact with the atoms present in the sample creating different type of signals that contain information about the surface composition and electrical conductivity. The electrons are emitted from a cathode of tungsten or lanthanum hexaboride (LaB_6) by applying a difference of potential (0,5-30 KV). This difference of potential allows the electrons to be accelerated from the anode. The objective lens adjusts the beams of electrons before they reach the sample analyzed. Tungsten is normally used because of its high melting point, the highest of the metals, and its lower steam pressure allowing to be heated for the electrons emission. The bundle of electrons has a very small focal point between 0,4-0,5 nm.

This characterization technique is very useful as it provides high resolution images and three - dimensional appearance that helps to analyze and characterize the surface. SEM was applied in this work to evaluate the morphology of the surface of the cathodes or layers and to identify the cathodes components (before and after cycling).

3.3.2 XRD

X-Ray diffraction is a common technique used in the characterization of cathode materials. The focus is the identification of crystalline components, the determination of structural properties, the degree of crystallinity and the quantification of different phases. An X-ray diffraction pattern is like a fingerprint for each substance.

In this investigation, this technique was used to identify sulfur and determinate its crystalline structure. The X-ray patterns were measured with D8 Discover X-Ray diffractometer with an area detector VanTEC 2000. Each diffraction pattern was measured in four frames with a step size of 23°, starting with $\Theta_1=\Theta_2=12°$. The exposure time for each frame was 180 s.

4. Results and Discussion

4.1 Degradation of the batteries during cycling

One of the biggest problems of lithium sulfur batteries is the high degradation during cycling. Figure 14 a) shows the variation of discharge capacity up to 50 cycles. These results were obtained from testing batteries built with standard cathode (50% sulfur, 40% CB and 10% PVDF) and standard electrolyte E_0 (1M of $LiPF_6$ in TEGDME).

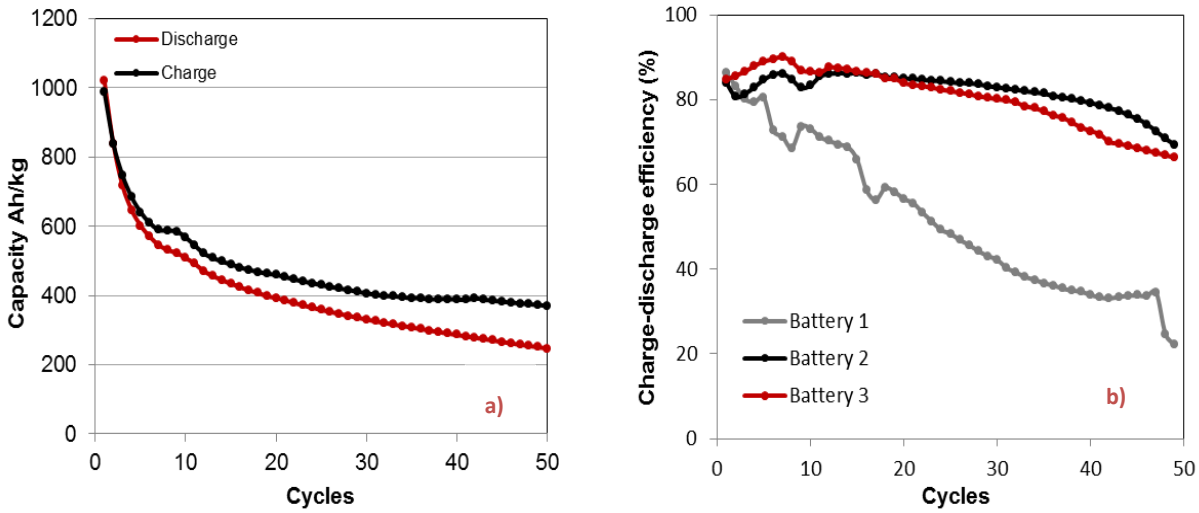

Figure 14: a) Charge and discharge curves for one of the standard batteries; b) Charge-discharge efficiency for all standard batteries tested.

As it can be seen in Figure 14 a) the discharge capacity decreases until approximately 247 Ah/kg and the charge and discharge curves are not overlapping. Figure 14b) shows the charge-discharge efficiency curves. These values were obtained from the following equation:

$$C_{eff} = \frac{D_{n+1}}{C_n} \times 100$$

where, D is the discharge capacity, C the charge capacity and n the number of cycle.

The charge-discharge efficiency decreases with the number of cycles, which is in agreement with the results expected from Li-S batteries according to literature (Mikhaylik, 2010). The discharge capacity decreases more than 50 % after 50 cycles.

The charge capacity is, in all the cases, larger than the discharge capacity and these differences increase during cycling (from 23 % until 30 %). This can be explained by the fact that the long chain reactions that

take place in these batteries retard the formation of the high structured sulfur (S_8). This may occur because soluble polysulfides migrate through the electrolyte from the cathode to the anode and react directly with the lithium metal retarding the reaction: $Li_2S_8 + 2e^- + 2Li^+ \rightarrow S_8 + 2Li$ or not allowing the reactions to continue until the formation of S_8. This process happens for all the cycles of discharge and charge and it is known, as mentioned before, as shuttle mechanism. Normally the capacity in the first cycle is high but it decreases sharply for the second cycle.

The following results show the curves of discharge and charge upon cycling for one of the above mentioned batteries.

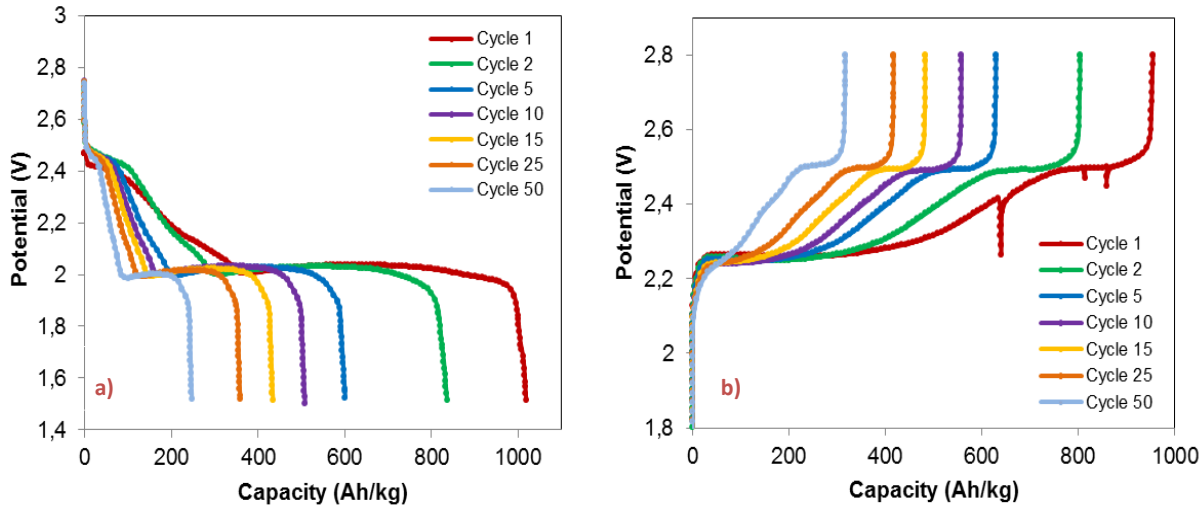

Figure 15: a) Discharge capacity curve; b) charge capacity curve

Figure 15a) shows that the major loss of capacity occurs during the first cycles of the battery. From cycle 5 to cycle 50th the capacity loss is more stable, for example, the loss of capacity between cycle 2 and 5 is 28 % and from cycles 10 to 15 is 14 %.The discharge curve presents two plateaus, one at higher voltage (~2,5 V) and other at lower voltage (~2 V). By the charge curve the first plateau appears at~2,2 V and the second appears at ~2,5 V. These results are in agreement with the information presented in the chapter 2 of this work.

The results from the x-ray diffraction test of the standard cathode are shown in the following figures 16 and 17. This analysis was performed with the main objective of characterizing the structure of the cathode as the rays establish contact from the surface of the cathode until the substrate.

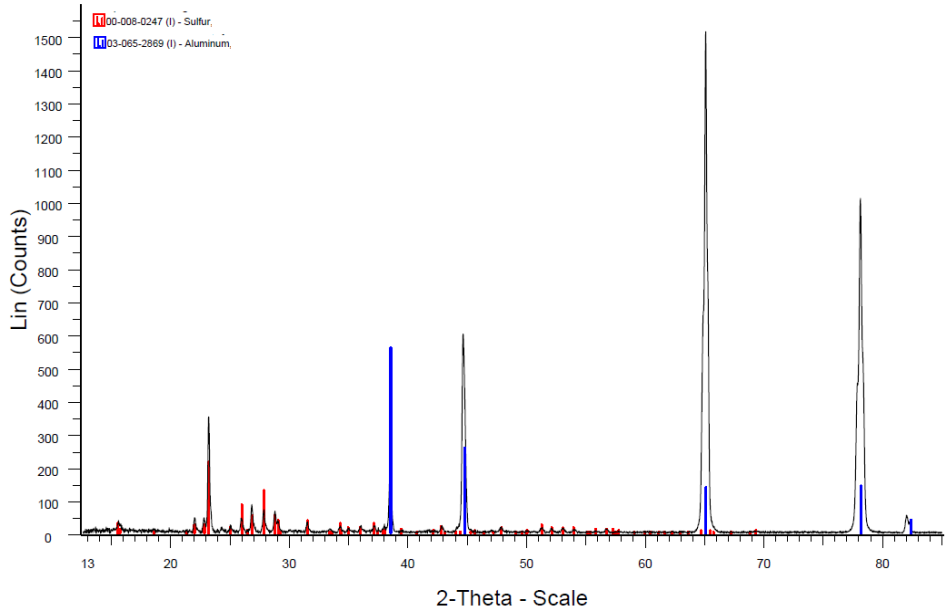

Figure 16: XRD pattern of the standard cathode before cycling

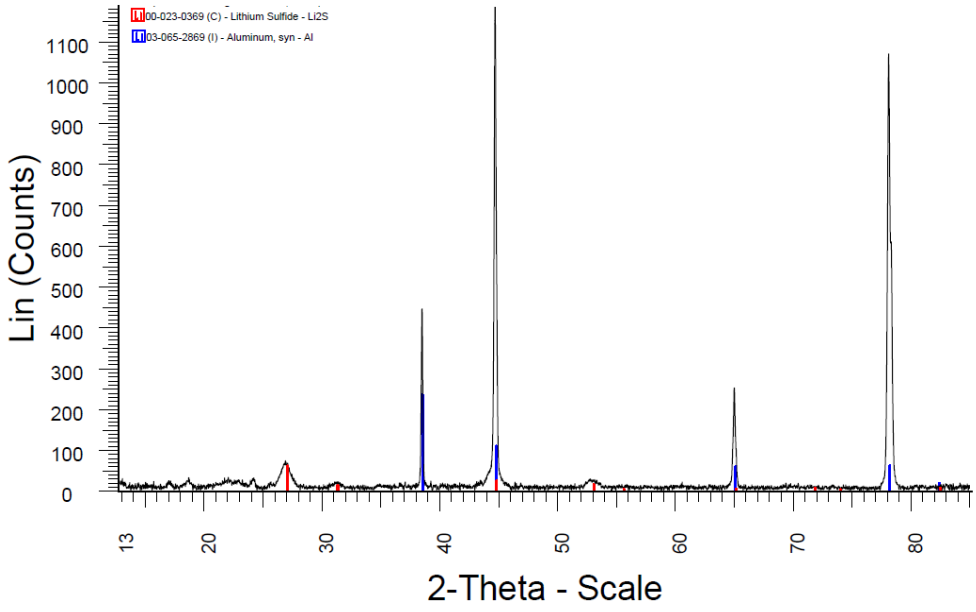

Figure 17: XRD pattern of the standard cathode after one discharge.

By the analysis of the previous figures it is possible to see a difference in the peaks of each diffraction patterns. Before cycling, (see Figure 16) reflexion peaks of sulfur and aluminum (from the substrate) can be identified. The structure of sulfur is S_8 orthorhombic face-centered.

Figure 17 shows the standard cathode after one discharge (from an in-situ measurement). Here, it is possible to see that the sulfur is not present but Li_2S appeared. These results are in agreement with the literature as the sulfur totally disappears after cycling (Lixia Yuan, 2009).

4.2 Suspension mixture: mechanical mixing vs. ultra sound mixture

After the first test with the ultra sound mixing, the resultant suspension was applied over an Al-foil and dried. The resulting cathode mixture was characterized by means of SEM. The results are shown in Figure 18.

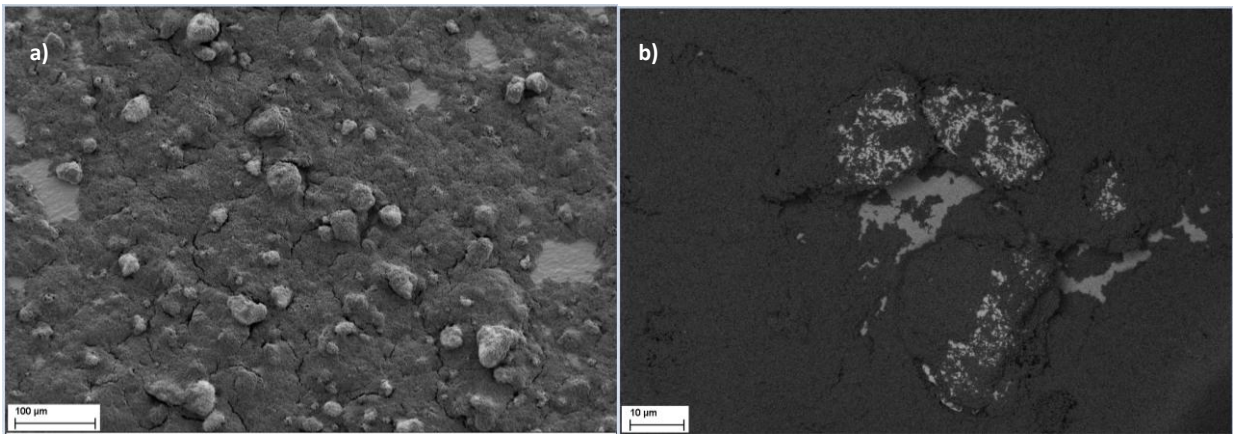

Figure 18: a),b) SEM micrographs of the cathode surface from the suspension prepared with the US mixer for two different scales.

In these pictures, it can be seen that the size of sulfur particles is high, more and less, between the ranges of 15-20 µm. Figure 18b) also shows that some particles are not totally covered with carbon black. Due to the size of the particles and the observation of agglomerates in the suspension itself, the spraying was not performed since the nozzle could be blocked. As it shown in Table 1 the suspension where tested with different amplitudes. It could be seen that the suspension mixed at 100 of amplitude presented less agglomerates than the other mixed with lower amplitude.

In order to avoid these results the ultra sound mixture procedure was changed. In a second ultra sound test, 50 % of the solvent (PVDF and PEG already dissolve in it) was added to the sulfur and then mixed with ultra sound mixing for the time presented on Table 1 (only for amplitude of 100). After the sulfur and solvent were mixed the same procedure was applied for carbon black. Finally, sulfur, carbon black and solvent were mixed together for the same time conditions mentioned in Table 1.

As the particles and agglomerate size were not small enough for spraying, it was necessary to change the procedure once again. In this third experiment, it was necessary to mix the solvent first as it had big particles of PVDF. This may have happened because PVDF absorbed some humidity that changed the properties of this component and made it difficult to dissolve in solution. After this step the sulfur was mixed 30 % with the solvent and the carbon black was mixed with the other 70 %. Less percent of solvent is needed for sulfur, because it could be seen that sulfur dispersed easily in the solvent, while carbon black not. In this case the sulfur was mixed with the solvent for about 5 minutes and after that

the carbon black was mixed for about 35 minutes as shown in Table 1 always at amplitude of 100. After, the sulfur, carbon black and solvent were mixed together for the same time as shown in Table 1. In the following SEM figure the results of test 3 are presented.

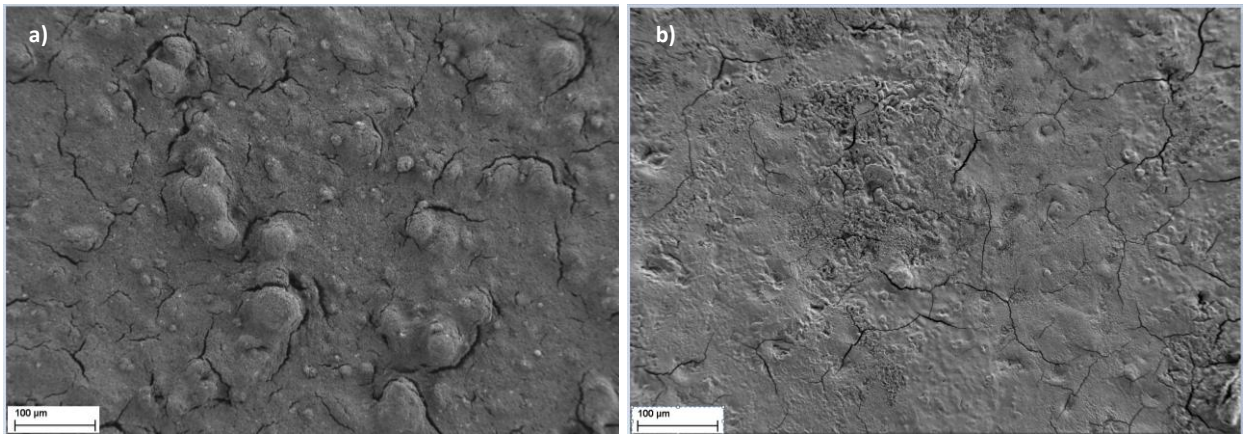

Figure 19: a) Surface of the US cathode before cycling; b) surface of the US cathode after cycling

As it can be seen by analyzing Figure 19a),b) the suspension surface prepared with the ultra sound mixer has many cracks. This can be related to the DMSO slow evaporation after spraying as this cathode was thicker than the cathode prepared with the mechanical mixer. Figure 20a) shows SEM pictures of the sprayed cathodes from the suspension sprayed by mechanical mixing. Here no cracks can be seen.

It can also be seen that after cycling (Figure 19b)) the surface of the cathode was significantly covered with a solid film and the sulfur particles cannot be identified.

The size of the particles resulted from test 3 was lower than the previous suspensions but yet higher than the suspension prepared with mechanical mixing as shown in the SEM images presented in Figure 20). This fact can be explained based on the type of mixing used. In the mechanical mixing, four ceramic spheres were used to help mixing the solution. At the same time these spheres confer a grinding effect, disintegrating agglomerates and reducing the sulfur particles size.

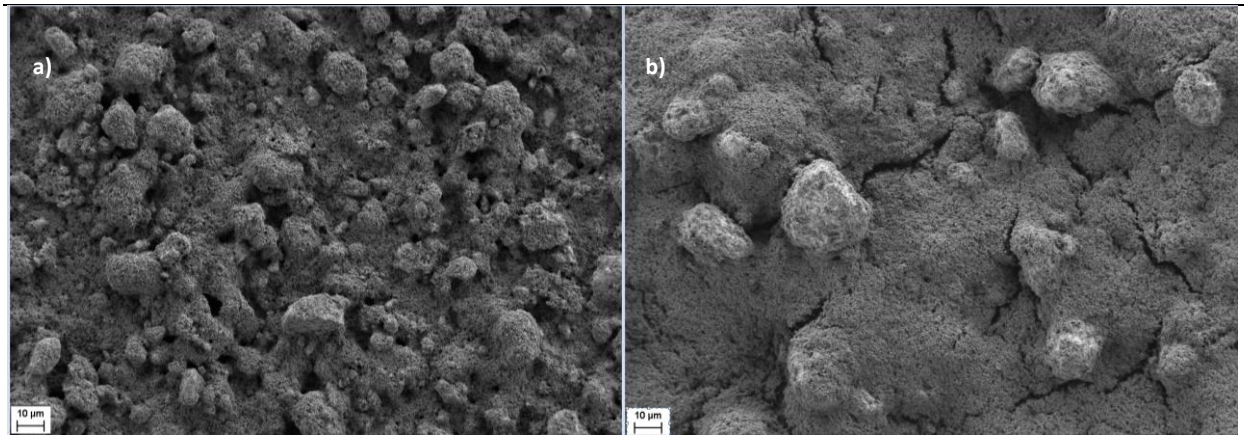

Figure 20: a) Surface of the cathode prepared with mechanical mixing; b) surface of the cathode prepared with ultra sound mixing

The suspension from test 3 was finally sprayed with the conditions presented in Table 2. While spraying the suspension in the substrate, it was possible to see that the layer formed on the substrate was not as homogeneous as the one prepared by mechanical mixing. This can be a result of agglomerates presented in this system. The cathodes resulting from this procedure were also tested in batteries for comparison with standard batteries. The curves of discharge capacity and charge-discharge efficiency for the ultrasound batteries and for the standard batteries are presented in Figure 21. These results are based in the average of three batteries. The standard deviation was also calculated to support the analysis of the reproducibility of these results.

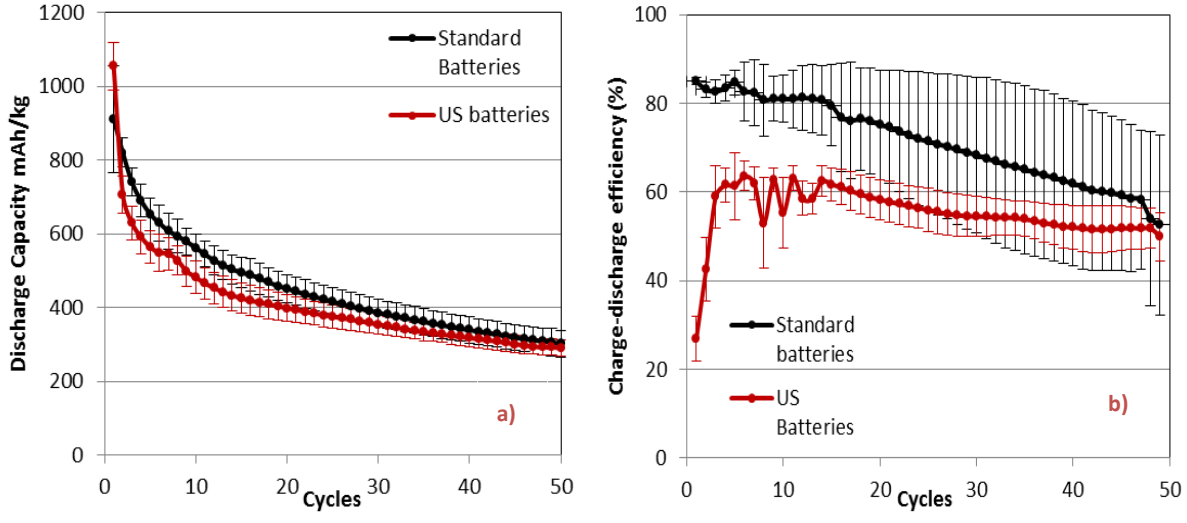

Figure 21: a) Discharge capacity for the ultrasound and standard batteries; b) charge-discharge efficiency for the ultrasound and standard batteries

The discharge capacity of US batteries is lower than the discharge capacity of the standard batteries during cycling. This lower capacity could be explained by the agglomerates presented in the US

suspension that hindered the sulfur utilization. The initial discharge capacity of the US batteries is higher but at the end they present the same capacity.

Figure 21b) shows the charge-discharge efficiency curves. The charge-discharge efficiency values are very different when comparing both curves. For the US batteries these values are much lower and also unstable. This could be explained by the fact that the surface of the cathode was not very homogeneous and the agglomerates, as shown in Figure 20 b), contributed to the instability of the cathode during the discharge and charge reactions.

4.3 Cathode protective layer

The cathode protective layers were built with the objective of protecting the cathode from the shuttle mechanism as they present great cationic exchange properties that difficult the migration of the polysulfides into the anode side and contribute to alleviate the shuttle mechanism (Holger Schneidera, 2012).

As mentioned before two layers with different compositions were built and the cycling performance was compared. These layers were also characterized by means of SEM in order to have a better understanding of their morphological structure. Moreover, they were tested not only before but also after cycling to verify if the layer was still present and protecting the cathode. These results are presented in Figure 22.

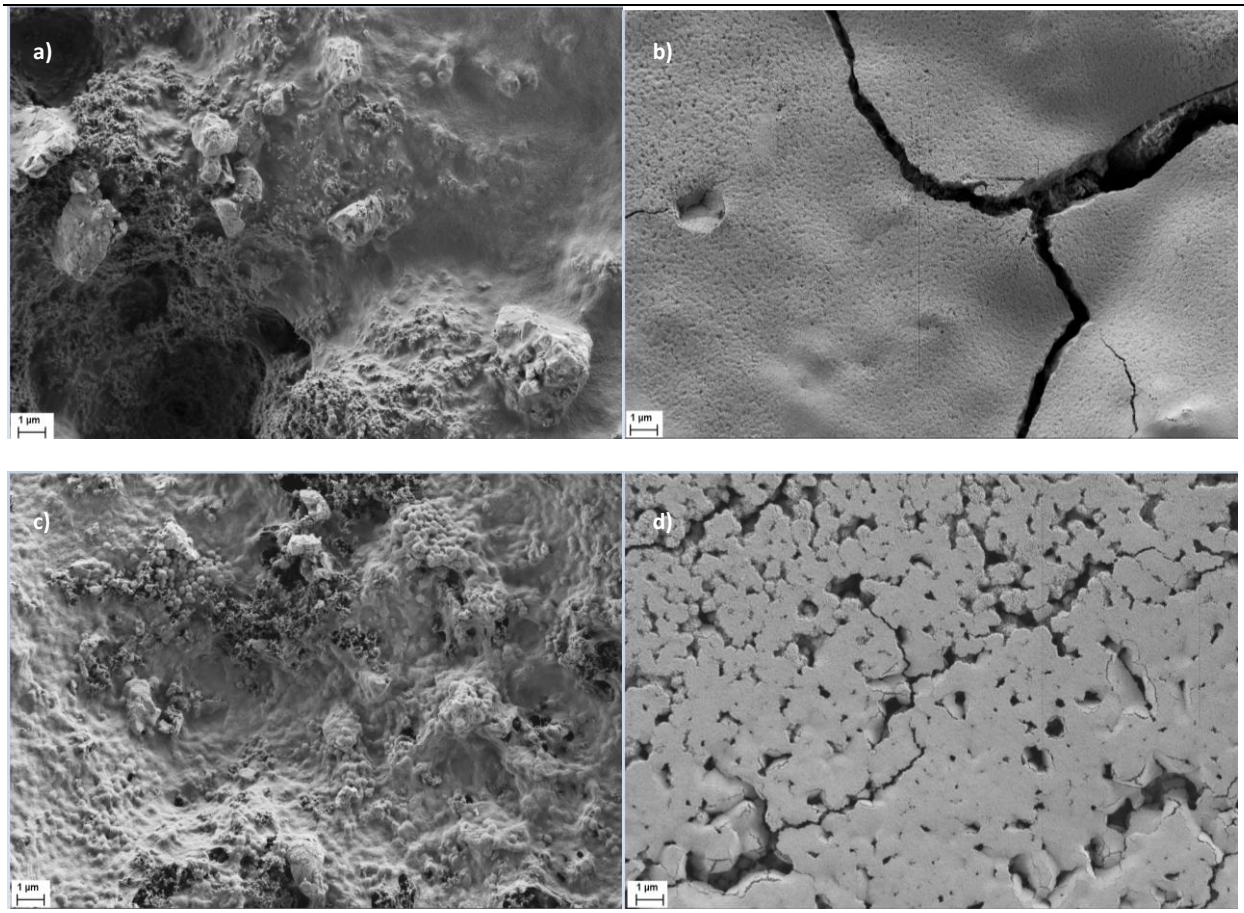

Figure 22: SEM pictures of (a) Layer L_a before cycling and (b) after cycling; (c) layer L_b before and (d) after cycling

By the observation of Figure 22a), c) it is possible to see the LiCGC particles as they have bigger size and high structured form. PVDF is binding LiCGC particles with the surface of the cathode and forming a thin layer that covers most of the sulfur and carbon black particles. Layer L_b seems to cover the cathode more than L_a.

After cycling, the morphology of the cathode changed. Figure 22b) shows that the surface is composed with cracks or cavities that probably were formed during the sulfur active material dissolution (Holger Schneidera, 2012). Figure 22d) shows the surface covered with a layer that formed during cycling. Compared with layer L_a, layer L_b does not show large cracks but some pores that can be seen on its surface.

The cathodes with these protective layers were tested in batteries in order to investigate if the shuttle mechanism was being avoided. In Figure 23 the results from testing these batteries in the BaSyTec are presented.

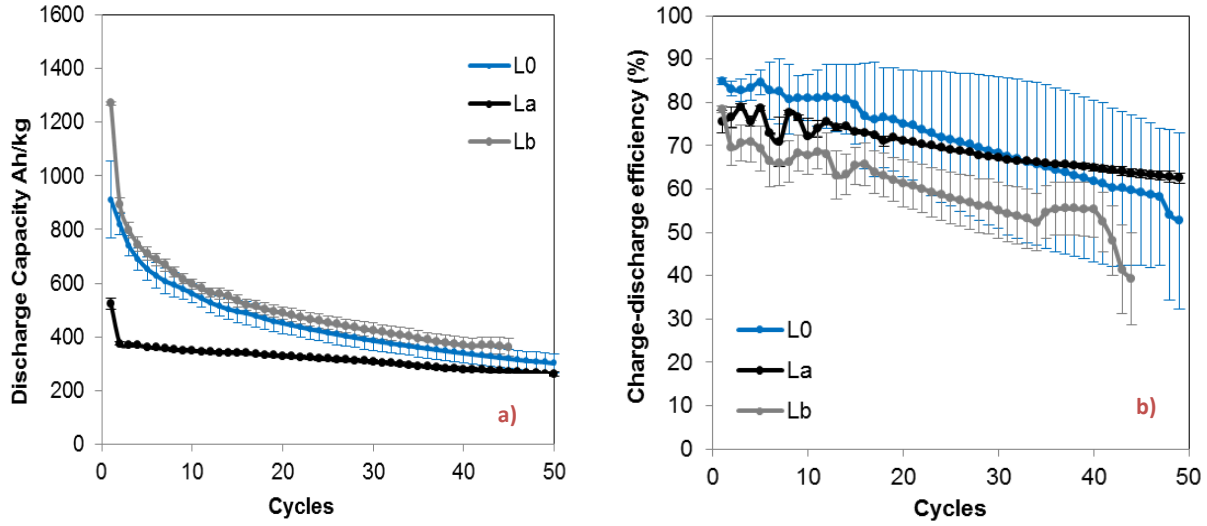

Figure 23: a) Discharge capacity for the different sprayed protective layers; b) charge-discharge efficiency for the different sprayed protective layers where, L_0 is the cathode with no protective layer for both plots.

As it can be seen in the previous plots, the batteries with L_b have a slightly higher discharge capacity then the battery with no layer (L_0) but at the same time the discharge capacity of both L_a and L_0 decreases significantly upon cycling. This means that these protective layers are not protecting the cathode from the shuttle mechanism as the discharge capacity still decreases. With the layer L_a the initial capacity is very low but at the same time this layer presents great stability from the 2nd cycle as the loss of capacity between the cycles 2 and 50th is 30% for the protective layer L_a and 79% for L_b. This represents a significant difference in the stability of each layer. The charge-discharge efficiency is very similar for all the layers. By the charge-discharge efficiency curves it is possible to conclude that the shuttle mechanism is also taking place in all the batteries because these values are much lower than 100%.

4.4 Influence of $LiNO_3$ as additive: effect of different electrolyte compositions

As mentioned before, the electrolyte is one of the most important components of a battery as it helps to conduct the ions through the separator from the anode to the cathode. Furthermore, it can influence the formation of solid electrolyte interface (SEI) on the anode depending on the additives used. Many electrolyte additives have been study for Li-S batteries but $LiNO_3$ is the additive which has led to the best results in this field. For this reason this additive has been tested in this work for different concentrations until the optimal concentration was found.

Table 5 shows the different concentrations of the electrolytes tested in this work. In figure 24, the results from one of the batteries tested with a concentration of 0,1 M of $LiNO_3$ additive are presented.

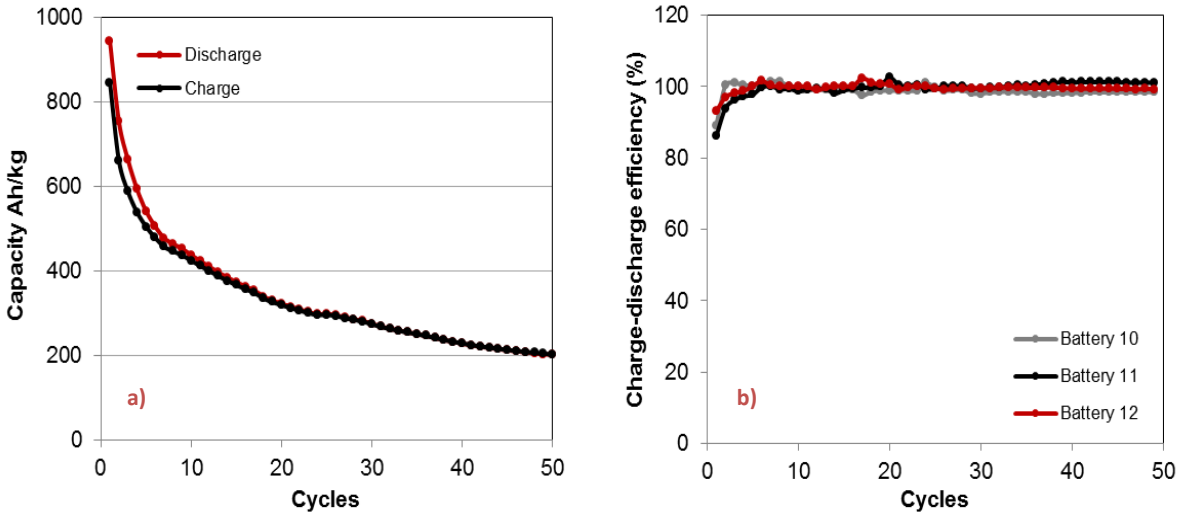

Figure 24: a) Discharge and charge capacity curves for the one of the batteries tested with E_3; b) charge-discharge efficiency for all the batteries with E_3.

These batteries with a concentration of 0,1 M of $LiNO_3$ additive present a significant different from the standard batteries as they have more stability as showed by both curves (see Figure 24a)). Figure 24b) also shows the high stability of the charge-discharge efficiency for all the batteries. This might result from the inhibition of the shuttle mechanism as the charge-discharge efficiency is about 100 from the 5th to the 50th cycle. As the discharge capacity still presented high degradation during cycle it was essential to change the concentration of this additive. For this matter, other electrolytes were created with concentrations from 0,5 - 2 M. The best results achieved were with electrolyte 4 with a concentration of 0,75 M. In the images shown in Figure 25, the batteries tested with this electrolyte are shown.

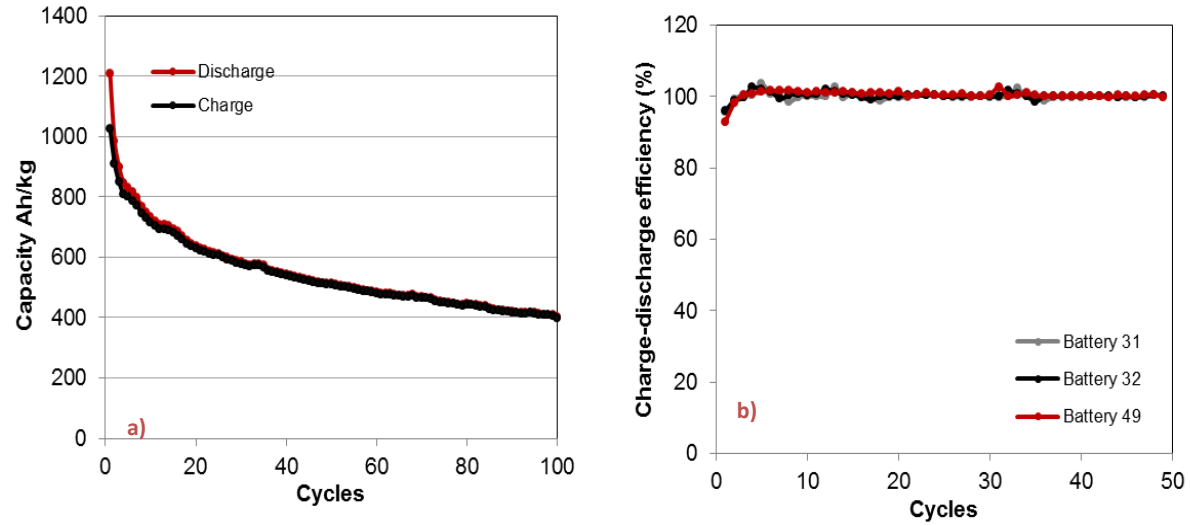

Figure 25: a) Discharge and charge capacity curves for one of the batteries with E_4; b) charge - discharge efficiency for all the batteries with E_4

Figure 25a) shows that the capacity in the 50th cycle is approximately 536 mA/kg. This is a significant improvement when comparing to the standard battery presented in Figure 14a) as the gain in capacity is 289 mA/kg (53 %). This curve has a significant loss of capacity in the first ten cycles, which is probably a consequence of the loss of sulfur in dissolved polysulfides or precipitated sulfur that is no longer in contact with carbon particles. Afterwards the capacity stays approximately constant. The charge – discharge efficiency curves are all very similar, stable and they reach the 100% in the 2nd cycle.

In order to identify the cause of the improvement of the results with electrolyte 4, this was studied by means of SEM and XRD.

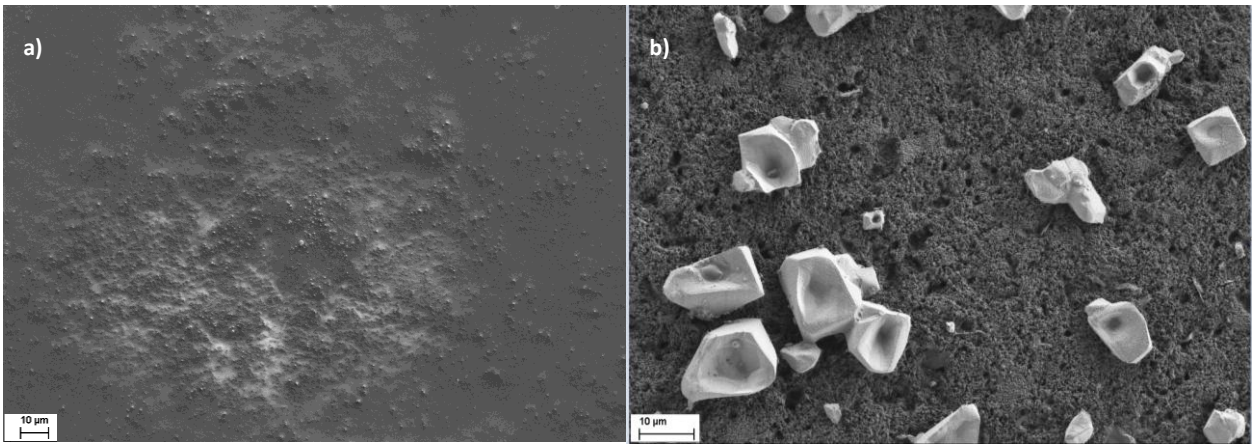

Figure 26: SEM images of the cathode surface after cycling for batteries built up with E_0 (a) and with E_4 (b).

In Figure 26 (b), it is possible to see that even after the 50 cycle particles of sulfur are still present. This kind of crystalline formation has not been seen for the standard cathodes after cycling (see Figure 26 (a)). Normally the surface of the cathode after cycling is covered by an amorphous layer of active material. For the case of the battery built up with electrolyte 4, the sulfur may recrystallize after 50 cycles. The morphology of the cathode could not be investigated in the bulk of the material, making difficult to assume that the same crystallites are still distributed in all the cross section of the cathode. Electrolyte 4 may enhance the reaction of the end products, S_8 and Li_2S. This may be an explanation why sulfur particles are still present in the sample after cycling. According to the literature after the first discharge the sulfur disappears from the surface and it is not possible to see by SEM micrographs (Lixia Yuan, 2009).

In Figure 27, as a support to these results, a XRD pattern of the same cathode is shown. When comparing the standard cathode before cycling with the cathode with E_1 it is possible to verify that the crystalline sulfur disappears with cycling as there are no peaks presented in this pattern. The cathode tested with electrolyte 4 (after cycling) shows some peaks with less intensity and some new Braggs peaks by small angles.

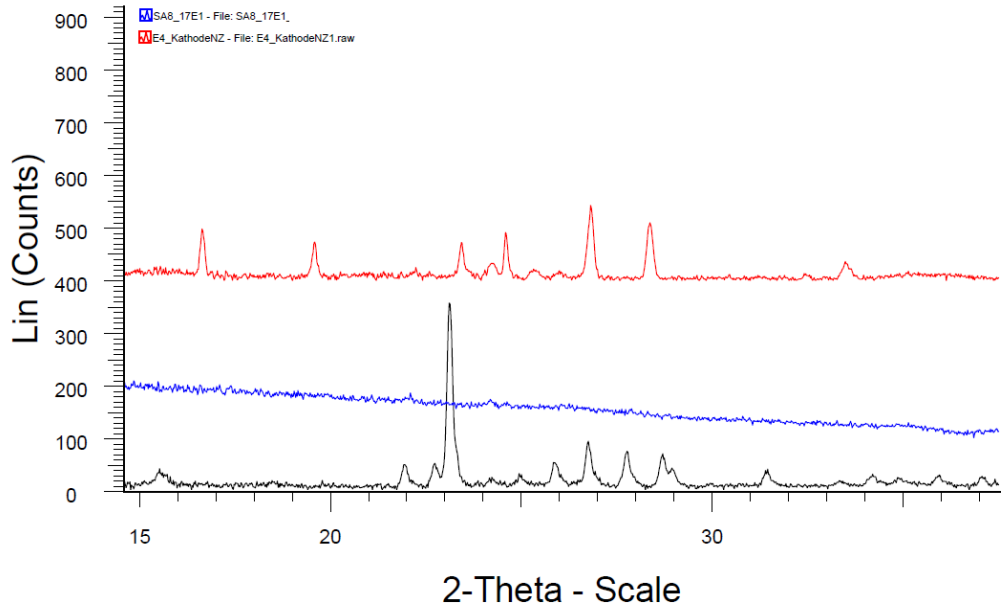

Figure 27: Patterns for one of the batteries with electrolyte E_4 (red), with electrolyte E_1 (blue) and for the standard battery before cycling.

This pattern has been fitted and the analysis display that a mixture of monoclinic and orthorhombic structure of sulfur are presented. These results are in agreement with the SEM pictures of the battery with electrolyte 4 presented before as they both show sulfur particles after cycling.

Figure 28 shows the results of EIS measurements for electrolyte E_0 and E_4 before cycling. E_0 has two semicircles at low and high frequencies. The high frequency semicircle usually is explained by the Li-ion migration through the SEI films, and the low frequency semicircle by charge transfer (probably across the passive film) (Lixia Yuan, 2009). E_4 presents a higher resistance than E_0 at high frequencies and the semicircle at low frequency cannot be seen.

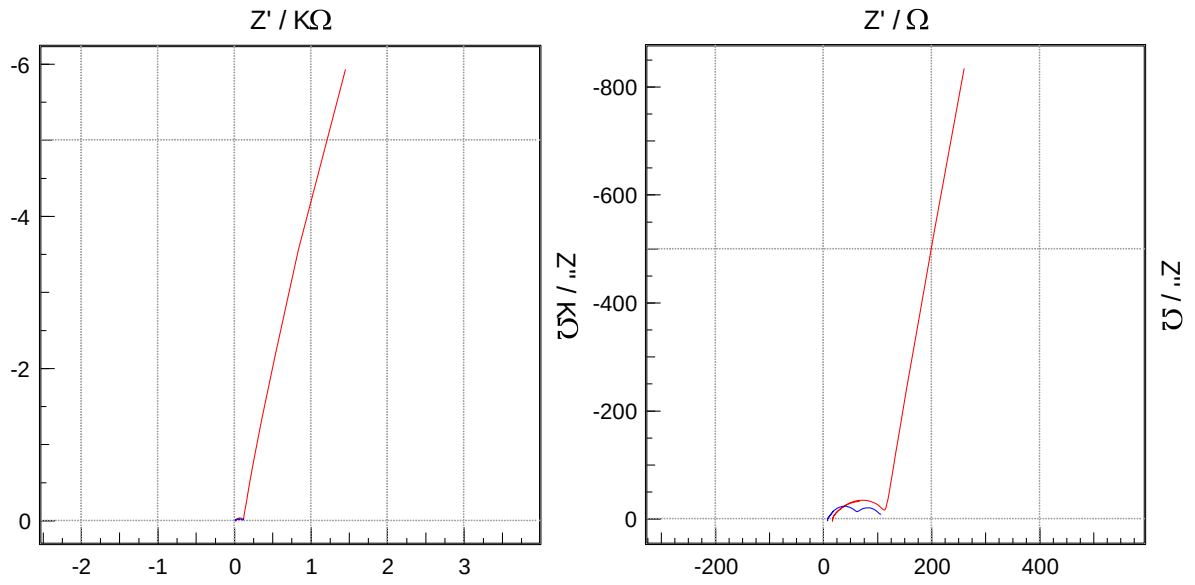

Figure 28: EIS spectra of electrolyte E_0 (blue) and E_4 before cycling (red). (a) Frequency range: 60 mHz – 1 MHz (b) Frequency range: 1 Hz – 1 MHz.

After 50 cycles, battery charged, the spectra of both batteries illustrate a higher resistance at high frequencies. In the case of $E_{0,}$ the resistance at low frequencies increases more than the one at high frequencies. For electrolyte E_4 a semicircle at low frequencies appears. This can be explained by the formation of a layer in the anode side during cycling that increased the charge transfer.

Although a lower resistance in the battery is observed with E_0, it has more degradation during cycling. The increasing of resistance by E_4 may be a justified by the formation of a more stable protective layer that reduces the shuttle mechanism (see Figure 29).

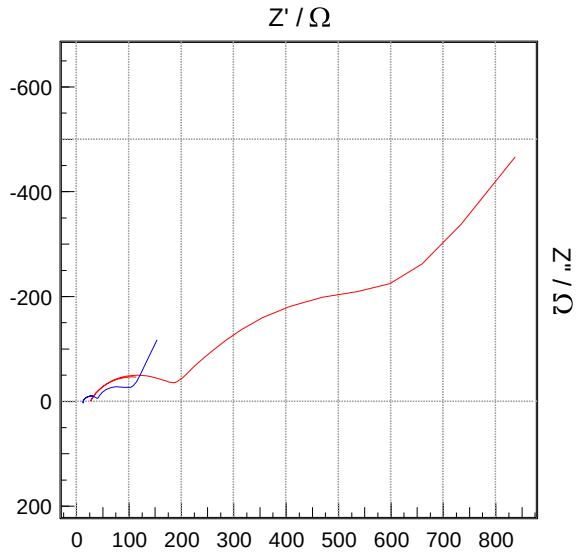

Figure 29: EIS spectra of electrolyte E0 (blue) and E4 (red) after cycling.

Figure 30 summarizes the capacity performance of all electrolytes during cycling.

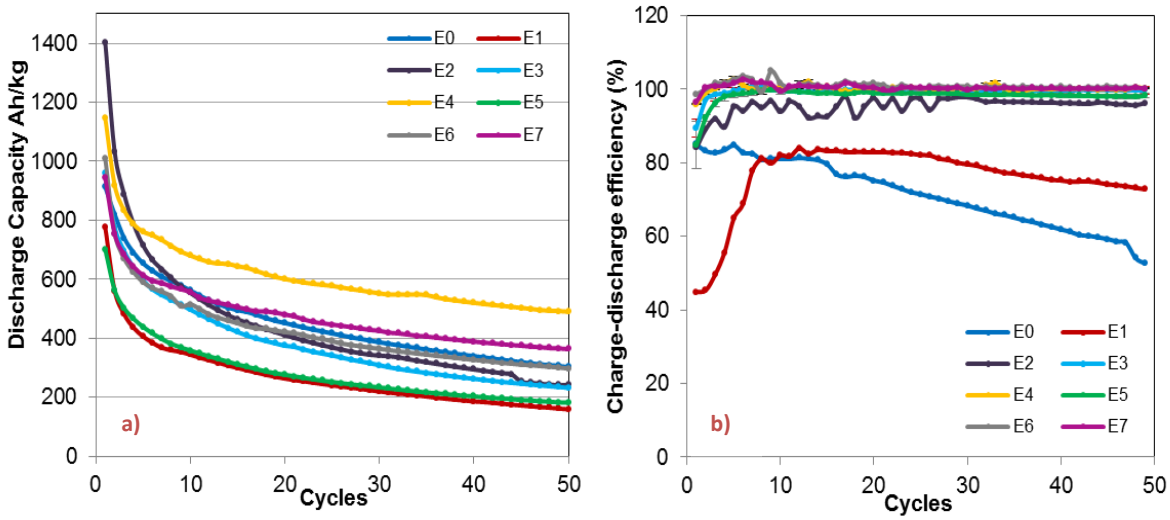

Figure 30: a) Discharge capacity from the batteries with E_0-E_7; b) charge-discharge efficiency for the batteries with E_0-E_7

The batteries with a concentration lower than 0,1 M are very unstable. In the charge-discharge efficiency curves this instability is also shown as the values are lower than 100 %. This means that the reactions occurring during the discharge are not the same that occur during charge, by other words the shuttle mechanism is not being avoided.

Batteries built with E_2 present high initial capacities, about 1400 mA/kg. This value is close to the theoretical capacity (1672 mA/kg). However, they still present high degradation during cycling. With electrolyte E_4 it is possible to see a significant difference in the discharge capacity when comparing to the other electrolytes. This proves that the shuttle mechanism in these batteries is avoided by, for what is believed, to be the formation of a protective film on the anode. This protective layer allows the transfer of lithium ions to the electrolyte during charging, but may avoid the reaction of polysulfides directly with lithium. In this way, polysulfides are not reduced in the anode during charging and they can oxidize in the cathode until the formation of sulfur is completed.

It is important to mention that electrolyte 8 was also tested for three batteries but they stopped working around the 4thcycle so the results are not going to be showed here but as index in the additional information chapter.

A bar graphic is shown above to a better analysis and comparison of the electrolytes (Figure 31).

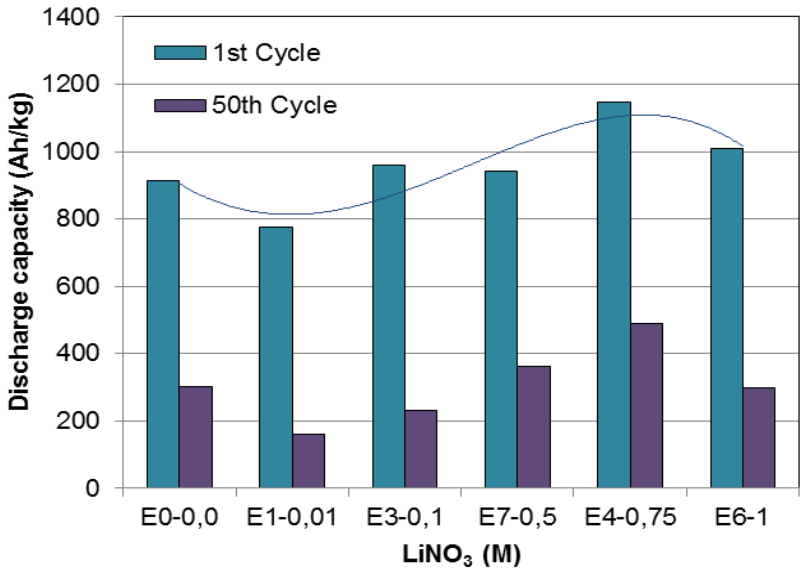

Figure 31: Discharge capacity for some of the electrolytes tested representing only the values for the 1st and 50th cycles.

The optimal concentration for the electrolyte additive is 0,75 M of $LiNO_3$. For this concentration the highest discharge capacity is reached after the first and fifty cycles. This figure also shows that concentrations of $LiNO_3$ between 0,5 to 0,75 M results in significant improvement when comparing to the standard electrolyte.

4.5 Combination of the protective layers with the best electrolyte

This part of the work has, as a main objective, the optimization of the results as it combines the best electrolyte with the two different protective layers of the cathode created. With this, it is intend to achieve higher specific capacities in the beginning and decrease the high degradation of the battery during cycling as these batteries have a layer protecting the cathode and supposedly a layer that forms with the lithium nitrate additive protecting the anode. For this purpose three batteries were made with the L_b and with electrolyte 4. The results are plotted in the Figure 32.

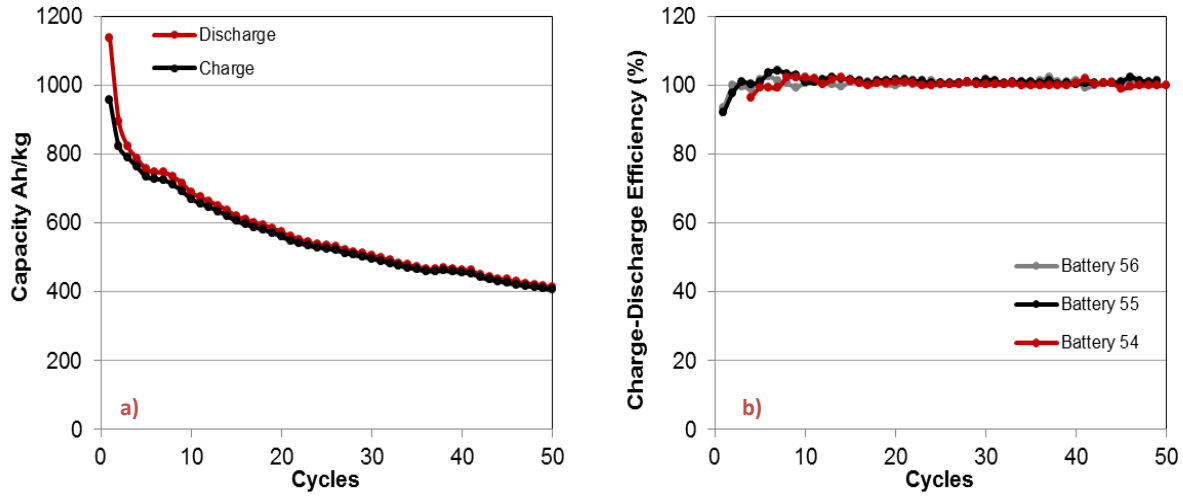

Figure 32: a) Typical charge - discharge curve for one of the batteries with E_4+L_b; b) charge-discharge efficiency curve for all the batteries with E_4+L_b.

When comparing these results with the results from the protective layer L_b, it is possible to verify a difference in the stability of the batteries as the charge and discharge curves are overlapping and the charge-discharge efficiency curves are very similar and all stabilize at 100 %. In comparison with the batteries with just layer L_b these are better as their values of the charge-discharge efficiency were lower than 80%. However it is still verified a high decrease of the capacity lower than the batteries with electrolyte 4 which means that no improvement was achieved by mixing the electrolyte 4 with the protective layer L_b.

The next step was to build batteries that combined electrolyte 4 with L_a, as this layer shows great stability upon cycling. The results from this test are shown in Figure 33.

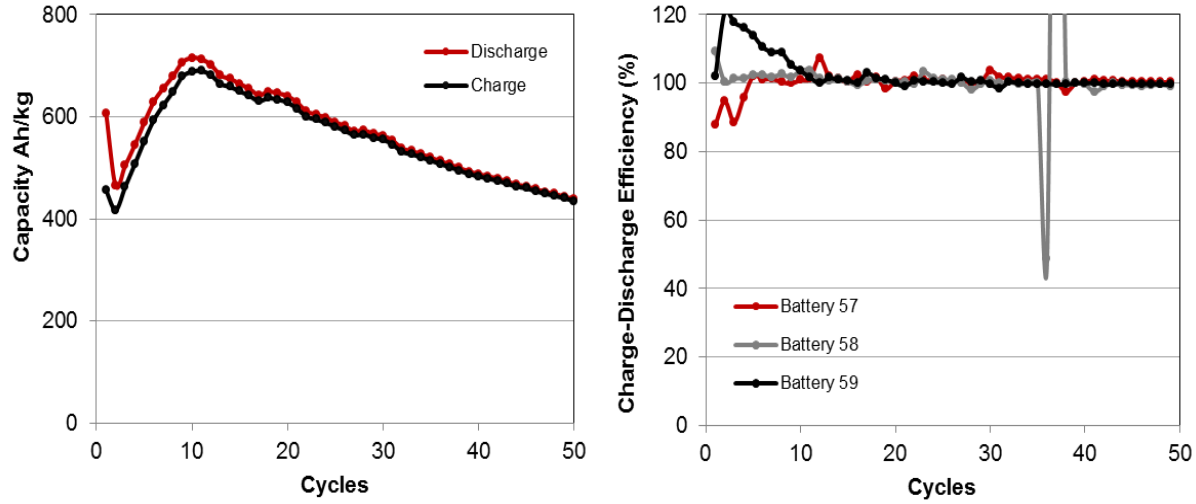

Figure 33: a) Discharge and charge capacity curves for one of the batteries with the electrolyte 4 and protective layer L_a; b) charge-discharge efficiency curves for all the batteries with electrolyte 4 and protective layer L_a

Figure 33a) shows that the battery is gaining capacity in the first cycles and then it decreases almost linearly. Figure 33b) illustrates the significant difference between the charge - discharge efficiency curves since for batteries 58 and 59 these values increase and decrease sharply. These results can be explained by the presence of cracks that are formed in the cathode during cycling (see Figure 22b)). These cracks or cavities lead to a higher utilization of insulating active material as it collapses into the crack formed getting in contact with the conductive additive and then leading to an increase of the capacity (Holger Schneidera, 2012). When comparing these results with the batteries with the layer L_a and the standard electrolyte it is possible to verify that the capacity in the last cycle is higher due to the increasing in capacity observed for the first cycles. In comparison with the batteries with electrolyte 4 it is possible to verify that the batteries mentioned before still present high degradation and in the end the discharge capacity is the same but yet it has a tendency to decrease almost linearly.

5. Conclusions

In this section the summary and conclusions of the work are presented:

- Ultra sound mixing was tested as a method for cathode suspension preparation and the parameters of mixing were optimized for this technique. In spite of decreasing the mixing time of the suspension, the ultra sound mixing has some disadvantages compared to the actual mechanical mixing. It requires more preparation steps, needs cooling during mixing and there is some loss of active material during the suspension preparation steps. Besides, the suspension has more agglomerates and no significant increase of discharge capacity was observed in the batteries. Therefore, this method will not be applied in future work, during the cathode preparation.
- Cathode protective layers composed of LiCGC and PVDF were successfully built. Layer L_a was proved to be very stable upon cycle as the capacity of this is approximately the same during cycling (between 400-300 mAh/gS). The loss of capacity between the cycles 2 and 50^{th} is 30% for the protective layer L_a and 79% for L_b which is traduced in a significant difference in the stability of the batteries.
- $LiNO_3$ was tested as additive for $LiPF_6$ (0,1 M) : TEGDME electrolyte. With the utilization of this additive at concentration higher than 0,1 M the charge –discharge efficiency reaches 100% and maintain constant during cycling. For this reason, it is believed that this additive reduce the shuttle mechanism occurring in this battery. The highest initial capacity was achieved for electrolyte 2 (1400 Ah/kg) close to the theoretical capacity (1675 Ah/kg) and the highest discharge capacity achieved was of 536 Ah/kg after 50 cycles for electrolyte E_4. The loss of capacity in the batteries with electrolyte E_4 between the first and the last cycle was increased in 195 Ah/gS compared with standard batteries.
- The combination of the cathode protective layer L_b with the new electrolyte E_4 resulted in no improvement in the capacity for these batteries. Nevertheless, for protective layer L_a, the capacity in the beginning is the same when comparing to the batteries with only the protective layer but increases in the first cycles and is higher for the last cycle (113 Ah/kg more).

5.1 Accomplished Objectives

- *Study the influence of $LiNO_3$ as additive in electrolyte ($LiPF_6$ in TEGDME) on the cycling stability of Li-S batteries*. This electrolyte was tested for eight different concentrations of the $LiNO_3$ additive. For each change in the electrolyte additive concentration, three batteries were made. This electrolyte additive was also studied by means of EIS and SEM.
- *Create a protective layer on the cathode to enhance sulfur retention and avoid morphological changes. Use of PVDF for coating and additional ion conductive salts, in this case $LiPF_6$, can be used in the polymeric matrix.* In this work two different protective layers of the cathode were created with different concentrations of LiCGC. They were sprayed in the cathodes and after they were tested in batteries for cycling.
- *Study the influence of ultra sound and mechanical mixing conditions during suspension preparation*. The ultra sound mixer was tested for three different amplitudes and during the time periods presented in Table 1. Also it was tested with three different procedures in order to optimize its mixing behavior.
- *Preparation of suspension for the cathode and spraying by means of air atomizing equipment*. This air atomizing equipment was used when spraying the suspension for the cathode on the substrate and when the protective layers were sprayed on the cathodes. This equipment was used twice for the spraying of the suspension in the substrate (SA8 and SA9).
- *Assembling and cycling batteries upon 50 cycles*. Some batteries were also tested for 50 cycles plus one charge and for 100 cycles.
- Characterization of the samples by means of:
    - *Scanning Electron Microscopy (SEM).* This method was very helpful in this work to characterize the surface morphology of the different samples. It was used to test the cathode prepared with the ultra sound mixer, to test the different layers that were made and also to identify which particles were present in the anode surface after cycling.
    - *X-Ray diffraction (XRD).* This method was very helpful when identifying the components that were present before and after cycling in the surface of the cathodes and also to verify that LiCGC was still present, after cycling, protecting the cathode.
    - *Electrochemical Impedance Spectroscopy (EIS).* This method was used to evaluate and compare the behavior of electrolyte 4 and the standard electrolyte.

5.2 Limitations and Future Work

More work has to be done in respect to the cathode protective layer as these were only the first steps taken on this subject. Other ion conductive materials such as Nafion could be used to increase the protective behavior and also other conditions when spraying could be changed in order to achieve better results. During spraying the protective layer, there were some difficulties due to the constant changed of the suspension pressure. Also the suspension overpressure was zero for the layer L_a. This was also a problematic procedure because when spraying with no pressure the suspension was not enough to reach the cathode. It is necessary to increase the protecting behavior because the cathodes morphology can be easily changed leading to an active mass loss.

More work has to be performed in the electrolyte in order to obtain less degradation of the batteries during cycling. For example, changes in the solvent of $LiPF_6$ and TEGDME or in the additive. As mentioned before, it is believed that the N-O bond is responsible for the inhibition of the shuttle mechanism. For this purpose other materials with this bond can also be tested.

References

- *www.ohara-inc.co*. (2012). Retrieved June 21, 2012, from www.ohara-inc.co: http://www.ohara-inc.co.jp/en/product/electronics/licgc.html

- Chang DR, Lee SH, Kim SW, Kim HT (2002). Binary electrolyte based on tetra(ethylene glycol) dimethyl ether and 1,3-dioxolane for lithium-sulfur battery. *J Power Sources* **112**(2)**:** 452-460.

- Chen JJ, Zhang Q, Shi YN, Qin LL, Cao Y, Zheng MS*, et al.* (2012). A hierarchical architecture S/MWCNT nanomicrosphere with large pores for lithium sulfur batteries. *Phys Chem Chem Phys* **14**(16)**:** 5376-5382.

- Hassoun J, Agostini M, Latini A, Panero S, Sun YK, Scrosati B (2012). Nickel-Layer Protected, Carbon-Coated Sulfur Electrode for Lithium Battery. *J Electrochem Soc* **159**(4)**:** A390-A395.

- Ji XL, Nazar LF (2010). Advances in Li-S batteries. *J Mater Chem* **20**(44)**:** 9821-9826.

- Kolosnitsyn VS, Karaseva EV (2008). Lithium-sulfur batteries: Problems and solutions. *Russ J Electrochem+* **44**(5)**:** 506-509.

- Mikhaylik Y (2010). Electrolytes for lithium sulfur cells. US Patent 7 842 421 B2.

- Schneider H, Garsuch A, Panchenko A, Gronwald O, Janssen N, Novak P (2012). Influence of different electrode compositions and binder materials on the performance of lithium-sulfur batteries. *J Power Sources* **205:** 420-425.

- Tudron FB (2004). Lithium–sulphur rechargeablebatteries: characteristics, state of development and applicability to powering portable electronics. *Proceedings of the 41st Power Sources Conference* .

- Wang WK, Wang Y, Huang YQ, Huang CJ, Yu ZB, Zhang H*, et al.* (2010). The electrochemical performance of lithium-sulfur batteries with LiClO4 DOL/DME electrolyte. *J Appl Electrochem* **40**(2)**:** 321-325.

- Yuan LX, Qiu XP, Chen LQ, Zhu WT (2009). New insight into the discharge process of sulfur cathode by electrochemical impedance spectroscopy. *J Power Sources* **189**(1)**:** 127-132.

- Zheng GY, Yang Y, Cha JJ, Hong SS, Cui Y (2011). Hollow Carbon Nanofiber-Encapsulated Sulfur Cathodes for High Specific Capacity Rechargeable Lithium Batteries. *Nano Lett* **11**(10)**:** 4462-4467.

Additional information

Cathode protective layer:

Cathode protective layers (L_a and L_b) tested by means of XRD:

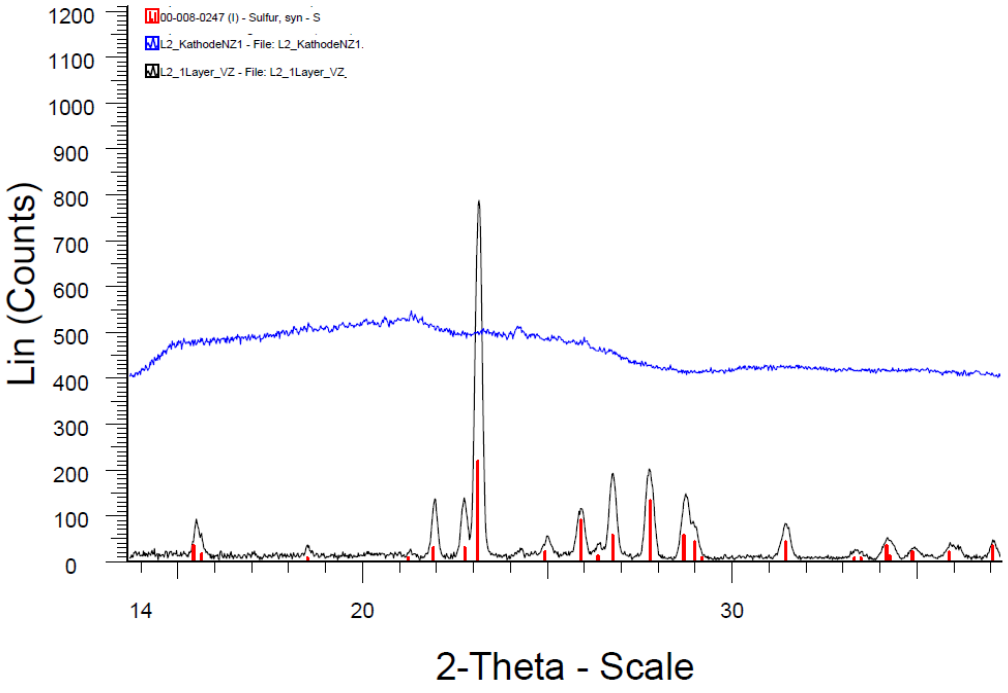

Figure 34: XRD pattern of the protective layer L_a before (black) and after cycling (blue).

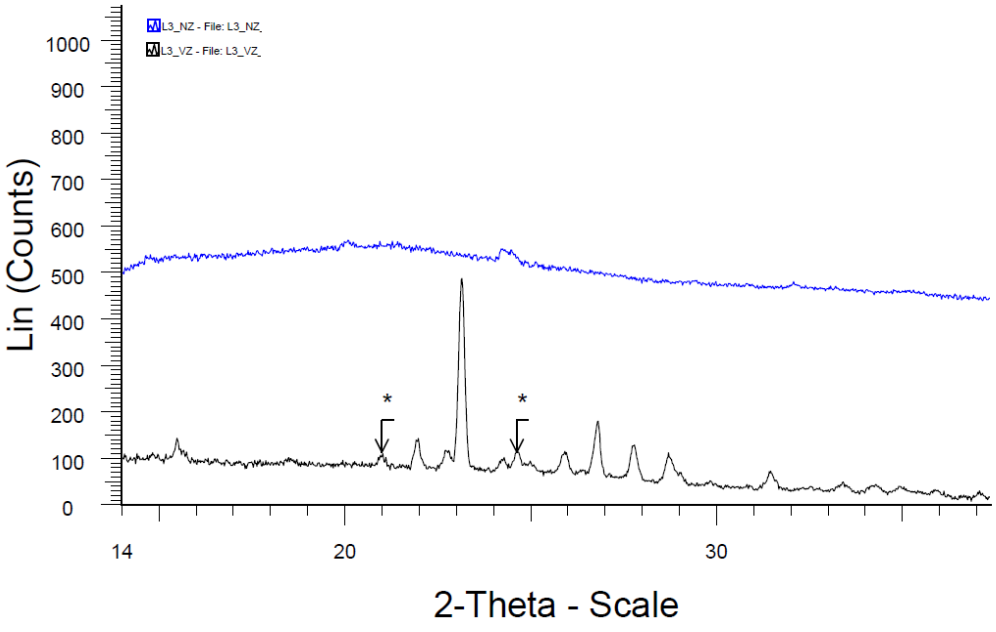

Figure 35: XRD pattern of the protective layer L_b before (black) and after cycle (blue).

Figure 34 shows the XRD pattern of layer L_a. Before cycling it is possible to see the sulfur particles and also LiCGC particles but with lower intensity peaks than in Figure 35 as the concentration of this compound was lower. After discharge no sulfur or LiCGC are identified, all components may become amorphous.

By observation of Figure 35 it is possible to observe that before cycle the LiCGC particles are present (peaks *). After 50 cycles (blue pattern) these peaks are not identified. The end product may be amorphous.

Layer L_b was mechanically pressed to increase the stability and adhesion to the substrate. This physical modification of the layer was only tested for one battery as its capacity was much lower than the batteries with the non-pressed L_b layer.

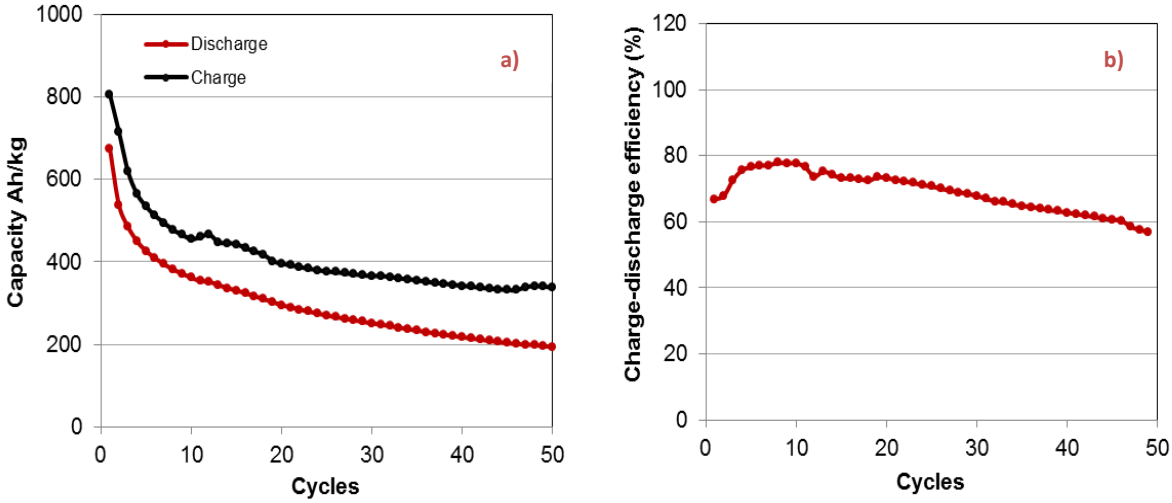

Figure 36: a) Charge and discharge capacity curves for the battery with pressed L_b layer b) charge-discharge efficiency for battery with pressed L_b layer.

The charge and discharge curves present lower capacity than the ones with the normal protective layer, but yet these curves are more stable than the ones that were not pressed. Also the charge discharge efficiency is very similar (lower than 80%) to the previous results (Figure 23).

Influence of $LiNO_3$ as additive: effect of different electrolyte compositions

The discharge capacity loss for the batteries with electrolyte 4 and the standard electrolyte (no additive) are going to be presented.

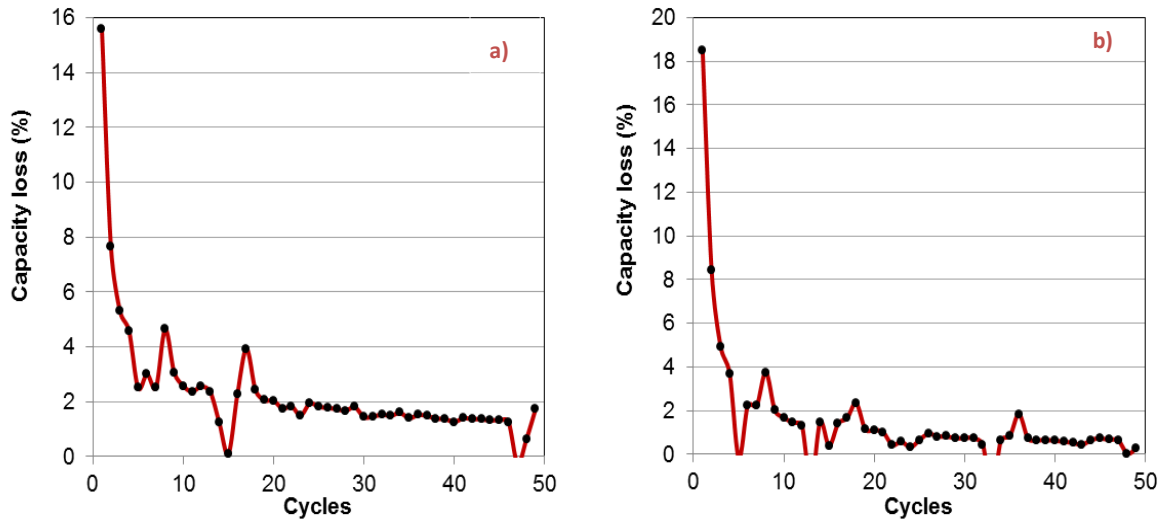

Figure 37: Capacity loss curves during cycling for battery with standard electrolyte E_0 (a) and for the electrolyte 4 (b) with 0,75 M of $LiNO_3$

The discharge capacity loss is lower for the batteries with the additive starting from the 5th cycle. The higher decrease in capacity is always verified from the first and the second cycle as the elemental sulfur is converted into polysulfides.

As mentioned before, electrolyte 8 (2 M $LiNO_3$), was also tested. However, these batteries did not show good performance during cycling, as only one battery of three reached 50 cycles.

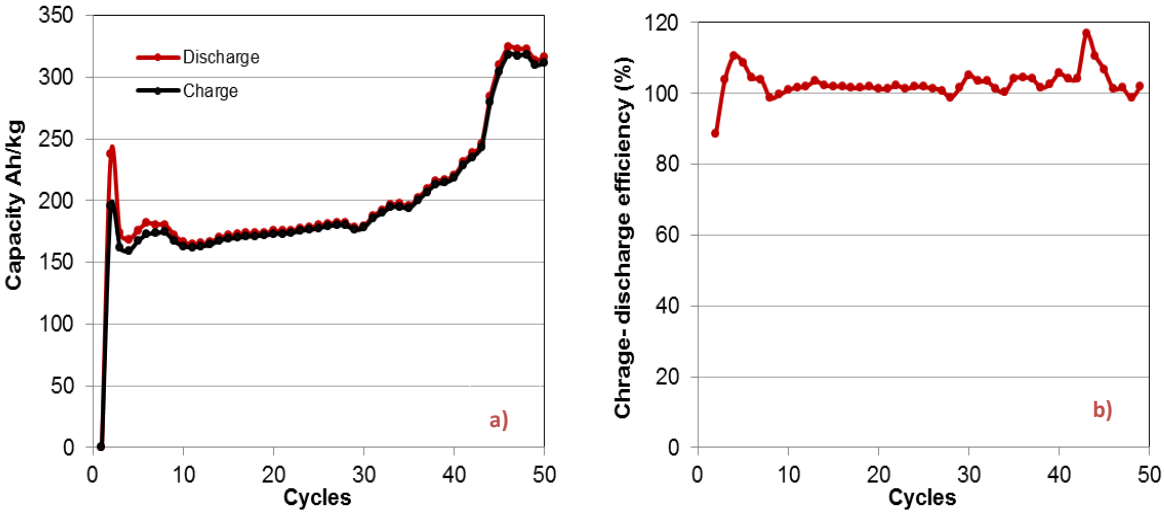

Figure 38: a) Charge and discharge curves upon cycling for the battery with electrolyte 8; b) charge discharge efficiency for the battery with electrolyte 8.

Furthermore the charge and discharge curves for batteries with electrolyte 2 and 3 with concentrations of $LiNO_3$ of 0,05 and 0,1 M, respectively, are going to be shown, due to their different plateaus form when comparing to the standard batteries.

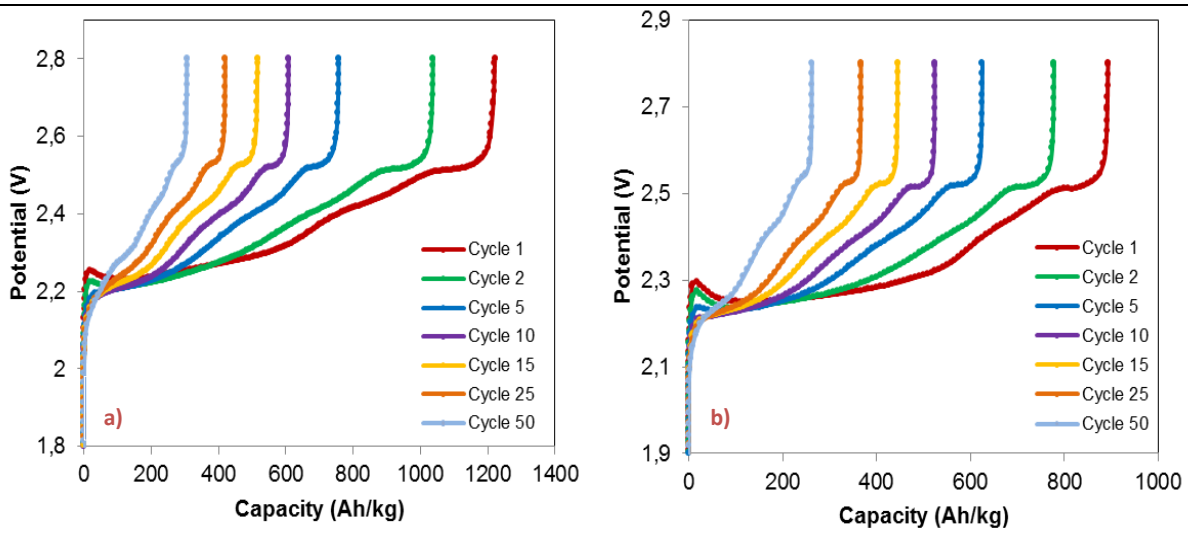

Figure 39: a) Charge capacity curve for one of the batteries with electrolyte 2; b) charge capacity curve for one of the batteries with electrolyte 3

The lower and higher voltage plateau is smaller than the curves shown in the literature and it is not very clear where it ends and where exactly starts the second one.

Lithium anode investigation

One of the challenges of the Li-S batteries is the difficulty in the characterization of lithium surface after cycling as this component reacts easily with air. However in this work, when disassembly of the batteries with the electrolyte 4 it was observed that some components were present in the lithium surface. For this reason, the lithium surface was rubbed with a conductive adhesive tape inside the glove box. After, it was transported to the laboratory where it was tested by means of SEM. These results are shown in the following figure.

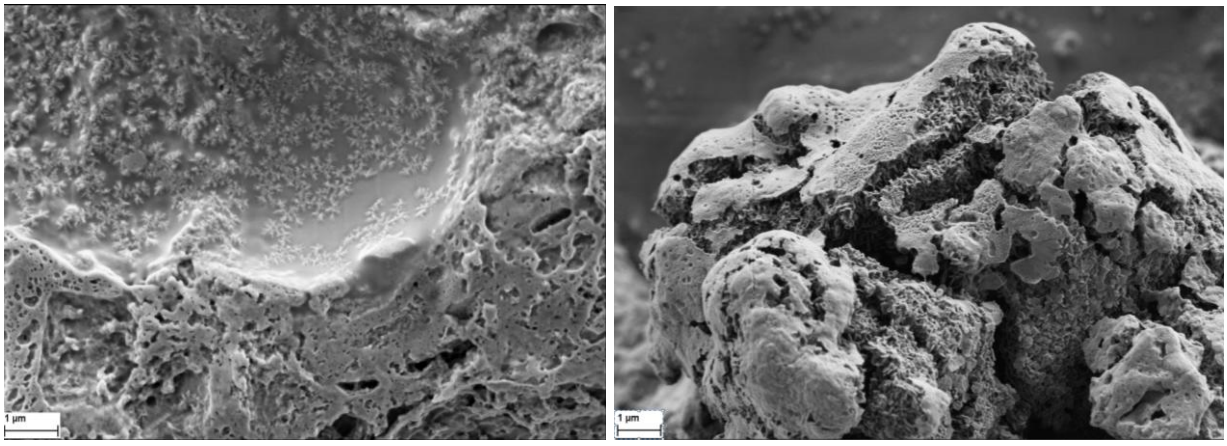

Figure 40: Structure of a component formed during cycling, on the lithium anode surface, after 50 cycles

Some crystallites and amorphous phases were formed during cycling in the anode surface. However, only with this test no conclusions can be made. For this matter this sample was tested after by means of XRD.

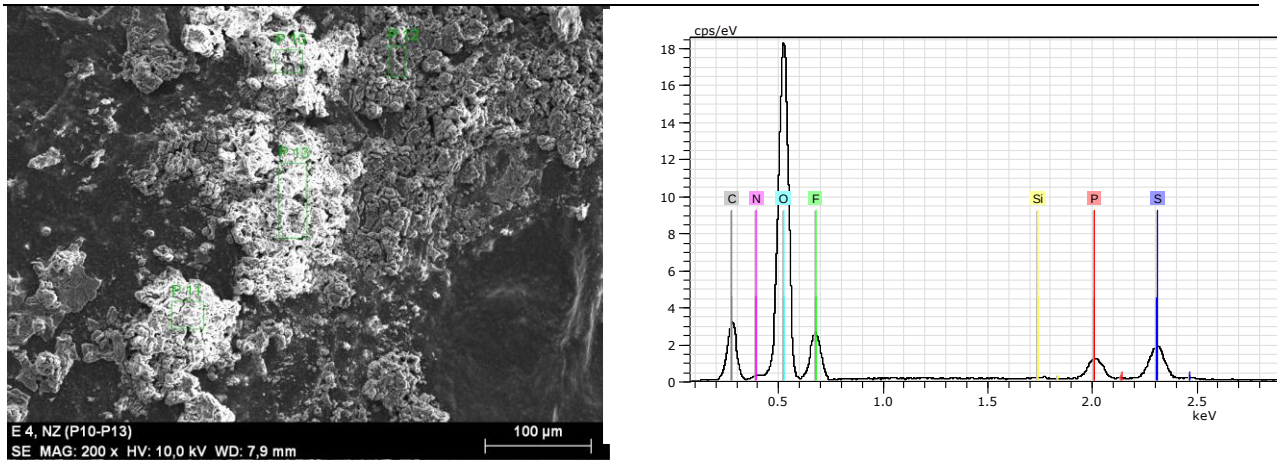

Figure 41: EDX analysis of the components on the surface of Li anode. P, S, C, O, and F are the elements that were identified in the region P13.

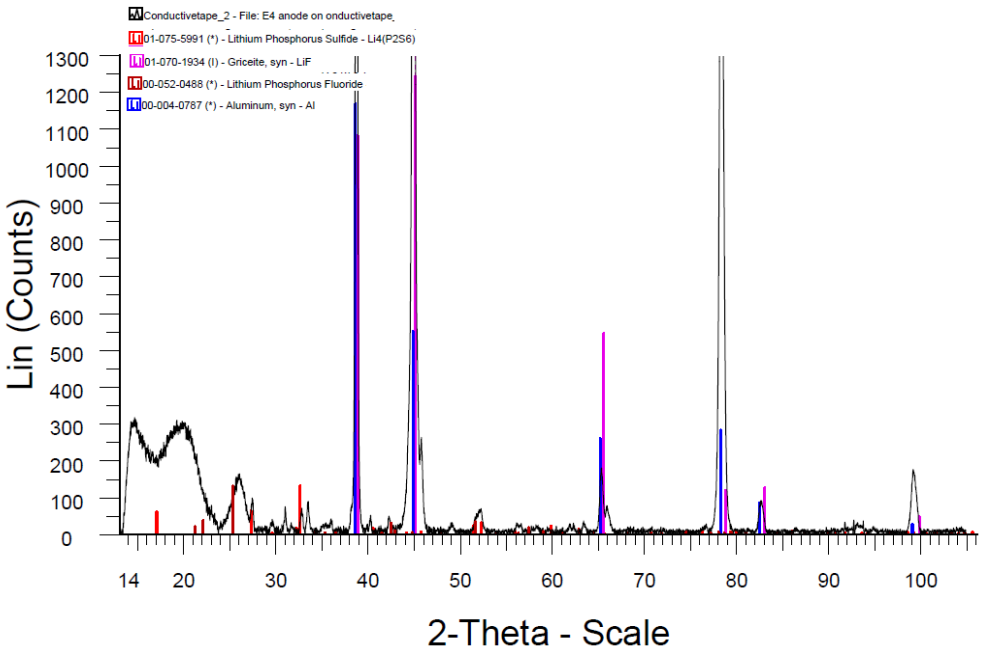

Figure 42: Illustrates the components pattern that were found in the surface of the lithium surface.

In this spectrum a new crystalline phase/s can be identified. Because of the low intensity of the peaks is difficult to confirm the exact composition of this component/s. Some measured spectra of possible candidates are shown: lithium phosphorus sulfide ($Li_4(P_2S_6)$), griceite/Lithium fluoride (LiF) and lithium phosphorus fluoride/ lithium hexafluorophosphate $LiPF_6$. The electrolyte may react with sulfur as the pattern for the $Li_4(P_2S_6)$ match some of the reflexion peaks.